DOI: 10.1002/ejic.200800771

1,2,4-Triazolium and Tetrazolium Picrate Salts: "On the Way" from Nitroaromatic to Azole-Based Energetic Materials

Thomas M. Klapötke*[a] and Carles Miró Sabaté[a]

Keywords: Azolium cations / Energetic materials / Explosives / Picrates

A family of energetic salts based on the picrate anion and several azolium cations were synthesized either by new methods or by known literature procedures. The cations of choice were the following: 5-amino-1*H*-tetrazolium (**1**), 5-amino-1-methyl-1*H*-tetrazolium (**2**), 5-amino-2-methyl-1*H*-tetrazolium (**3**), 5-amino-1,4-dimethyl-1*H*-tetrazolium (**4**), 5-amino-1,3-dimethyl-1*H*-tetrazolium (**5**), 1,5-diamino-1*H*-tetrazolium (**6**), 1,5-diamino-4-methyl-1*H*-tetrazolium (**7**), 3,4,5-triamino-1,2,4-triazolium or guanazinium (**8**) and 3,4,5-triamino-1-methyl-1,2,4-triazolium or methylguanazinium (**9**). A summary of the ^{15}N NMR shifts for all compounds is given, and the proton-/methyl-induced shifts (PISs/MISs) are discussed with relation to the crystal structures. Because hydrogen bonding plays an important role in determining the density and thus the performance of energetic materials, the crystal structures are discussed in detail. In addition, tests to assess the impact (*i*) and friction (*f*) sensitivities of the compounds and thermal stability measurements (DSC) were also carried out, revealing insensitive compounds ($i > 40$ J, $f > 360$ N) with high thermal stabilities ($T_d > 175$ °C). The constant volume energies of combustion were determined experimentally by oxygen bomb calorimetry and their validity was checked by quantum chemical calculation (MP2) of electronic energies. The detonation pressures and velocities of **1** (7795 $m s^{-1}$, 25.6 GPa), **2** (7343 $m s^{-1}$, 21.2 GPa), **3** (7213 $m s^{-1}$, 20.4 GPa), **4** (6876 $m s^{-1}$, 17.8 GPa), **5** (6846 $m s^{-1}$, 17.6 GPa), **6** (7864 $m s^{-1}$, 25.4 GPa), **7** (7492 $m s^{-1}$, 22.1 GPa), **8** (7495 $m s^{-1}$, 22.5 GPa) and **9** (7162 $m s^{-1}$, 19.8 GPa) were predicted by use of the EXPLO5 code. Lastly, the ICT code was used to predict the decomposition gases of all salts.

Introduction

Interest in high-energy density materials (HEDMs) continues.[1–7] New energetic compounds offering high performance and low sensitivity are sought for both military and civilian applications, though the two properties often play opposite roles.[8,9] The search for new and/or modified energetic materials that display the desired properties for use as pyrotechnics, propellants or high explosives is a continuing challenge. Classical energetic materials such as TNT (trinitrotoluene) or RDX (cyclotrimethylenetrinitramine) derive their energy from the oxidation of their carbon backbones,[10,11] whereas nitrogen-rich HEDMs owe their energies to their high positive heats of formation.[12,13] The explosive yield of TNT is considered one of the standard measures of strength of bombs and other explosives.[14] The compound has a relatively high detonation velocity and a high decomposition point.[15] The high thermal stabilities of nitroaromatic compounds are attractive for military applications. On the other hand, formal replacement of TNT's methyl group by a hydroxy group, as in the parent picric acid, results in detonation parameters better than those of TNT.[15] Picric acid, however, is more sensitive to classical stimuli (i.e., impact and friction) than TNT and accidents have occurred in the past. As an example, picric acid is known to react with surrounding metals (e.g., in a shell-casing) to yield very sensitive compounds. Not only is salt formation known to stabilize the materials through the formation of hydrogen-bonded networks,[16] but such compounds also tend to display lower vapour pressures and higher densities than their atomically similar non-ionic derivatives.[17] Whereas reports describing energetic nitrate, perchlorate or azide salts are becoming more common,[18] reports on energetic picrate salts are much more elusive in the literature. Recently, Shreeve et al. introduced a new family of mono- and bridged azolium picrate salts with prospective use as energetic materials,[19] although many of the compounds (e.g., 5-amino-1*H*-tetrazolium picrate) were not studied in detail from the energetic point of view. In addition to the latter work, there exist some structural reports of tetrazolium picrate salts,[19,20] but energetic data are scarce. Salts of picric acid, either with nitrogen-rich anions (e.g., ammonium or guanadinium) or with heavy metals (e.g., lead)[15] have interesting properties for use as explosives in military charges and as active components in initiating mixtures, respectively. In high-nitrogen chemistry, azole-based energetic materials are often the favourite choice, due to the reduced sensitivity and good thermal stabilities of

[a] Energetic Materials Research, Department of Chemistry and Biochemistry, Ludwig-Maximilians-Universität (LMU), Butenandtstr. 5–13 (D), 81377 München, Germany
Fax: +49-89-2180-77492
E-mail: tmk@cup.uni-muenchen.de
Supporting information for this article is available on the WWW under http://www.eurjic.org or from the author.

the resulting compounds, regardless of their many N–N bonds and relatively high performance.[21] We therefore decided to undertake an in-depth study of the energetic properties of picrate salts with triazolium and tetrazolium cations as intermediates between commonly used nitroaromatic energetic materials and (nitrogen-rich) azole chemistry (Figure 1). The nitrogen-rich azolium cation should contribute positively to the heats of formation and to enhanced densities. Lastly, in view of the negative oxygen balances of the picrates salts studied here, the energetic properties of mixtures of the materials with oxidizers such as ammonium nitrate or ammonium dinitramide were calculated in order to study the suitability of the mixtures as high explosives and/or propellants.

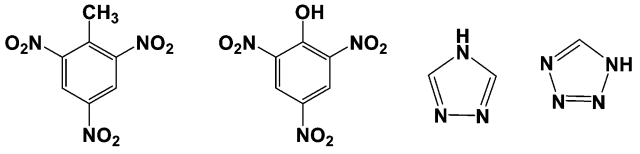

Figure 1. From left to right: formula structures of TNT, picric acid, 1,2,4-triazole and 1*H*-tetrazole.

Results and Discussion

Synthesis

5-Amino-1*H*-tetrazolium picrate (**1**),[19] 5-amino-1-methyl-1*H*-tetrazolium picrate (**2**),[59b] 5-amino-2-methyl-1*H*-tetrazolium picrate (**3**), 1,5-diamino-1*H*-tetrazolium picrate (**6**)[20a] and guanazinium picrate (**8**)[59a] were synthesized through reactions between equimolar quantities of the appropriate free bases and picric acid either in water or ethanol as the solvent. On the other hand, the synthesis of 5-amino-1,4-dimethyl-1*H*-tetrazolium (**4**),[59b] 5-amino-1,3-dimethyl-1*H*-tetrazolium (**5**),[59b] 1,5-diamino-4-methyl-1*H*-tetrazolium (**7**) and methylguanazinium (**9**)[59b] picrates proceeded through reactions between the appropriate azolium iodide salts and picric acid in boiling aqueous solution (Figure 2). The insolubilities of the products in the reaction solvent are the driving force for this reaction.

Lastly, apart from **8**, which is only slightly soluble in hot water but readily soluble in DMSO and DMF, the remainder of the compounds are readily soluble in hot water, DMSO, DMF and alcohol, whereas all materials are insoluble in less polar or nonpolar solvents such as acetone and ether.

Vibrational Spectroscopy

The vibrational modes of picrate salts **2**, **4**, **5**, **8** and **9** have already been described in a preliminary report from our group[59] and are therefore not considered in this section. As expected, both IR and Raman spectra are strongly dominated by the bands of the picrate anion. The asymmetric nitro group N–O stretching is observed as an intense band at 1565 (**1**), 1562 (**3**) and 1563 (**6** and **7**) cm^{-1} in the IR spectra and is inactive in the Raman spectra. The symmetric N–O stretching is observed in both IR and Raman spectra of the compounds. The differences between starting material (picric acid, PicH) and its salts are especially to be found in the Raman spectra, due to the splitting of the N–O stretch in many other peaks of high intensity and with maxima for the different compounds at the following wavenumbers: 1267 (**1**), 1261 (**3**), 1271 (**6**) and 1269 (**7**) cm^{-1} (IR) and 1296 (**1**), 1346 (**3**), 1348 (**6**) and 1334 (**7**) cm^{-1} (Raman). In addition, the IR spectra also show ring deformation modes for the anion at ca. 745 cm^{-1}. As for the cations, these show broad bands in the 3400–3100 [ν(N–H)] and 3000–2850 [ν(C–H)] cm^{-1} ranges in their IR spectra. The

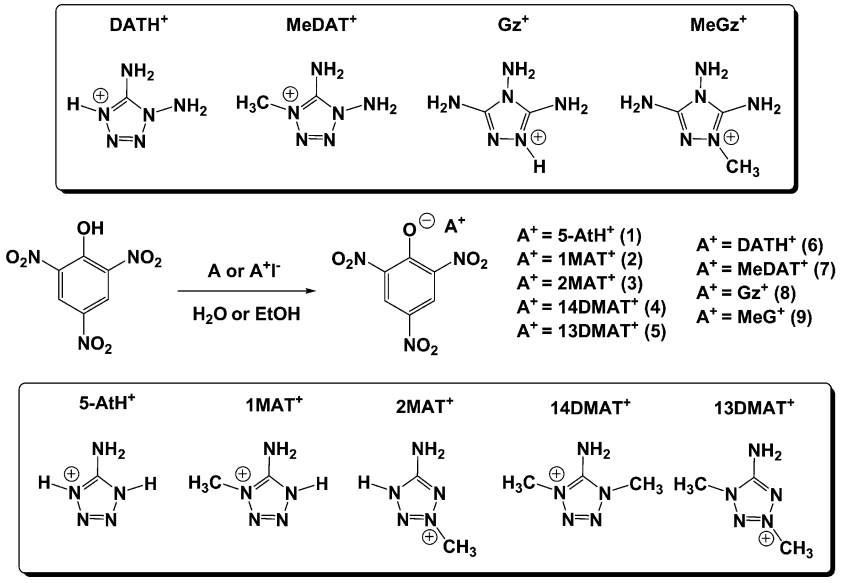

Figure 2. Reaction equation for the synthesis of azolium picrate salts.

IR spectra show bands of strong to very strong intensity in the range between 1696 (**3**) and 1722 (**6**) cm^{-1}, corresponding to the simultaneous elongation and deformation of the C–NH_2 and NH_2 bonds, respectively. The larger wavenumbers for **6** (1722 cm^{-1}) and **7** (1711 cm^{-1}) relative to the rest of the materials indicate stronger C–N bonds (i.e., more double bond character) in the *exo* carbon bound amino group, in keeping with structural reports on salts containing the cations **5**-At^+,[18b] $2MAT^+$,[22] DAT^+[18d,20a] and $MeDAT^+$,[18d,23] which display longer C–NH_2 distances. Lastly, many other bands of lower intensity are also present in both IR and Raman spectra of the salts and can be assigned as follows: 1550–1350 cm^{-1} [ν(tetrazole ring), $\delta_{as}(CH_3)$, δ(N–H)], 1380 cm^{-1} [δ(CH_3)], 1350–700 cm^{-1} [ν(N1–C1–N4), ν(N–N), γ(CN), δ(tetrazole ring)], <700 cm^{-1} [δ out-of-plane bend(N–H) $\omega(NH_2)$].[18c,24]

NMR Spectroscopy

As mentioned above, only the compounds not described in our preliminary reports[59] are discussed in detail here. In order to provide a better understanding of the importance of ^{15}N NMR as a characterization tool for azolium salts and to show the overall picture better, a summary of the NMR shifts for those compounds reported previously[59] is given, as well as those described here for the first time (Table 1).

The ^1H NMR spectra of the azolium picrate salts each show a sharp resonance at ca. 8.6 ppm corresponding to the aromatic protons in the anion. The N-1 methyl group protons (see Figure 4 for NMR labels) show similar shifts for all four cations in the 3.5–3.9 ppm range, whereas the N-3 methyl group protons in **3** are shifted to lower field (δ = 4.1 ppm). The different natures and acidities of the amino group protons in the picrate salts reported in this study can be observed in the ^1H NMR spectra. Compounds **1** and **7** have protons that are all very acidic, as suggested by their proton signals above ca. 9.0 ppm, whereas the rest of the compounds show (in general) averaged NH and NH_2 resonances, due to the fast exchange in the NMR solvent, at higher field.

Figure 3 shows the ^{13}C NMR spectrum of the new $2MAT^+$ cation in **3**. It is interesting to note that the formation of picrate salts results in a strong shift of the resonance of the carbon atom with the NMR label C-4 to high field (ca. 125 ppm) with respect to picric acid, and that this signal almost overlaps with that of the non-substituted carbon atoms (C-3/C-5). This is interesting because it confirms the formation of the picrate salts. Apart from the resonances for the aromatic carbon atoms in the anion in the ca. 125–160 ppm range (see Experimental Section),[25] the ^{13}C NMR spectra of the azolium picrate salts also each show the expected resonances for the cation. Analogously with the ^1H NMR spectra, the N3-substituted (NMR labels) compound

Table 1. ^{15}N and ^{13}C NMR chemical shifts (ppm), PIS/MIS values (ppm) and coupling constants (J) for the azolium picrate salts studied.

Compounds[a,b,c]	N-1	N-2	N-3	N-4	N-5	N-6	C–NH_2
5-At	–137.1	–13.1	–13.1	–137.1	–338.9	–	157.2
1	–168.1	–27.4	–27.4	–168.1	–326.2	–	155.0
	(–31.0)	(–14.3)	(–14.3)	(–31.0)	(12.7)		
					^1J 86.9		
1MAT	–185.3	–23.3	–2.0	–92.9	–339.4	–	156.4
2[d]	–184.2	–24.0	–12.9	–129.3	–331.1	–	155.1
	(1.1)	(–0.7)	(–10.9)	(–36.4)	(8.3)		
	^2J 1.9	^3J 1.6					
4[d]	–182.9	–29.3	–29.3	–182.9	–320.0	–	148.3
	(2.4)	(–6.0)	(–27.3)	(–90.2)	(18.2)		
		^3J 1.9	^3J 1.9				
2MAT	–116.1	–6.2	–83.0	–116.1	–339.3	–	167.7
3	–114.4	–9.0	–89.2	–114.9	–339.1	–	167.1
	(1.7)	(–2.8)	(–6.2)	(1.2)	(0.2)		
		^3J 1.4					
5[d]	–180.2	–31.6	–108.5	–110.3	–325.6	–	157.8
	(–64.1)	(–24.4)	(–24.5)	(5.8)	(14.7)		
		^3J 2.3			^1J 89.6		
DAT	–167.0	–5.5	–20.8	–97.5	–338.3	–315.2	155.0
6	–165.6	–20.9	–35.8	–173.8	–330.2	–320.1	153.1
	(1.4)	(–15.4)	(–15.0)	(–76.3)	(8.1)	(–4.9)	
7	–168.1	–24.2	–36.0	–186.9	–323.8	–312.1	147.4
	(–1.1)	(–18.7)	(–15.2)	(–89.4)	(14.5)	(3.1)	
	^2J 1.8		^3J 2.0	^2J 2.0		^1J 75.9	
Gz	–156.0	–156.0	–238.1	–340.2	–340.2	–326.4	152.1
8[e]	–177.1	–177.1	–238.9	–330.2	–330.2	–323.4	150.4
	(–21.1)	(–21.1)	(–0.8)	(10.0)	(10.0)	(3.0)	
9[d]	–239.8	–163.8	–238.3	–323.0	–335.2	–322.1	150.7, 147.7
	(–83.8)	(–7.8)	(–0.2)	(17.2)	(–5.0)	(4.3)	
				^1J 90.9	^1J 89.7	^1J 82.4	

[a] PIS/MIS values in curved brackets and coupling constants in Hz. [b] All shifts were measured with respect to CH_3NO_2 as internal standard; negative shifts are upfield from CH_3NO_2. [c] In [D_6]DMSO. [d] From ref.[59b] [e] From ref.[59a]

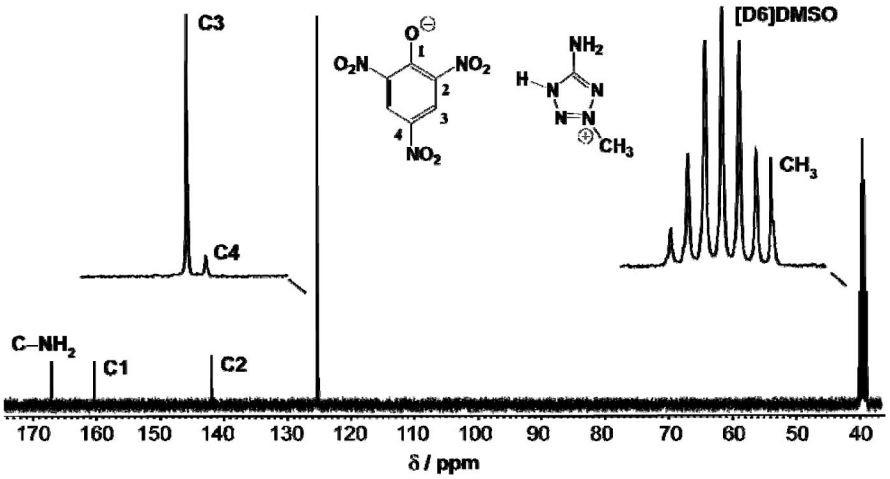

Figure 3. ^{13}C NMR spectrum of **3** in [D_6]DMSO with the assignments.

3 has a resonance for the tetrazole ring carbon atom (δ =167.1 ppm), which is at lower field than those of the rest of the compounds, whereas the 1,4-disubstituted tetrazolium salt **7** has the highest field shift for the same carbon atom (δ =147.4 ppm). The resonances for the methyl group carbon atoms vary over a relatively large range. The N3–CH_3 group in **3** has a resonance at δ = 38.8 ppm and overlap with the solvent (see Figure 3), whereas the N-1-bound carbon atom in **7** shows a high-field resonance at δ = 39.6 ppm.

The ^{15}N NMR spectra of ca. 0.2 M solutions of the azolium picrate salts in [D_6]DMSO show the resonances for the two picrate anion nitro groups at ca. –12 and ca. –15 ppm. These pairs of resonances coalesce into one and can already be observed in the ^{14}N NMR spectra at ca. –12 ppm, whereas the signals for the nitrogen atoms in the cation are broad. In addition to providing a quick method for unique identification of the picrate salts synthesized, protonation- and methylation-induced shifts (PISs and MISs) can also be used to obtain information about the structure and interionic interactions in solution. The PISs and MISs for the azolium salts described here can be calculated as the differences in ^{15}N NMR shifts between analogous nitrogen signals in neutral 5-At, 1MAT, 2MAT, DAT and Gz and the compounds. PIS and MIS values have been shown to be useful in determining the sites of protonation/methylation unequivocally for several heterocyclic compounds.[18d,26] Table 1 contains the ^{15}N NMR (and some ^{13}C NMR) shifts for all salts in this study, together with those of the corresponding neutral materials for comparison purposes, as well as the calculated PIS/MIS effects in brackets and the coupling constants (*J*; Figure 4).

Protonation of 5-At to yield the corresponding picrate salt (**1**) is accompanied by shifts (PISs) in the resonances of all nitrogen atoms (Table 1), which is more unexpected in the case of the protonated nitrogen atom (either N-1 or N-4) in keeping with the report on the crystal structure of the compound.[19] In a similar way, treatment of 1MAT with picric acid to yield **2** results in small PIS values in the range

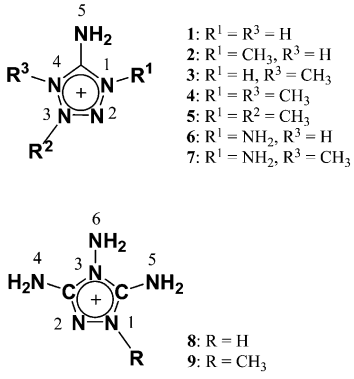

Figure 4. NMR labeling scheme for the tetrazolium and triazolium cations.

between –10.9 and +8.3 ppm for the nitrogen atoms N-1, N-2, N-3 and N-5 and a markedly larger value (–36.4 ppm) for N-4, indicative of protonation of this nitrogen atom, as is also confirmed by the crystal structure of the compound (see discussion below).[20b] Formal methylation, rather than protonation, of 1MAT to form **4**, results in MIS values between –27.3 (N-3) and +18.2 (N-5) ppm for all nitrogen atoms apart from the methylated one (N-4), which is shifted by –90.2 ppm with respect to the analogous nitrogen atom in 1MAT. Unexpectedly, the formation of **3** is not accompanied by large shifts in the resonances of the nitrogen atoms. Preliminary results involving the crystal structures of salts containing the $2MAT^+$ cation[22] showed protonation to take place on N-1; however, NMR studies do not conclusively support this observation and the expected protonated nitrogen atom (N-1) shows the largest positive (small) PIS in comparison with neutral 2MAT. A plausible explanation for this might be related with the relatively low basicity of 2MAT in the NMR solvent ([D_6]DMSO). Whereas the reaction between picric acid and 2MAT proceeds readily in water to form **3** (see Exp. Sect.), we observed that in less polar solvents (e.g., ethanol, CH_3CN or acetone), and possibly in [D_6]DMSO, picric acid (PicH) and

2MAT are recovered. We therefore conclude that the small PIS values observed for the ^{15}N NMR spectrum of the compound are due to the deprotonation of **3** to form 2MAT and PicH in the solvent used and over the large timescale of ^{15}N NMR measurement (in comparison with ^{1}H and ^{13}C NMR), which support formation of the salt. The MIS values for picrate salt **5** are lower than those for the majority of the compounds described here and vary between –24.5 (N-4) and +14.7 (N-5) ppm, and the methylated nitrogen atom (N-1) has the largest (negative) shift of all tetrazolium salts with a value of –64.1 ppm. Lastly, the diaminated salts **6** and **7** show PIS and MIS values of –76.3 and –89.4 ppm for the protonated (**6**) and methylated (**7**) nitrogen atoms, respectively, by comparison with DAT, whereas comparison of the shifts of neutral Gz with those of the triazolium salts **8** and **9** also shows relatively small MIS values between –0.2 and +10.0 ppm for the nonmethylated nitrogen atoms, whereas N-1 has the largest shift (PIS = –21.1 ppm for **8** and MIS = –83.8 ppm for **9**).

For the tetrazolium salts **1**, **2**, **4**, **6** and **7**, the nitrogen atoms with the labels N-2 and N-3 have ^{15}N NMR resonances at lower field (less negative), below –36 ppm. The other two tetrazolium salts (**3** and **5**) are exceptions to these low-field shifts, and the resonances for the methylated nitrogen atom (N-3) are observed at –89.2 and –108.5 ppm, respectively, due to the MIS effect. The amino group nitrogen atoms (N-5) are easily identified by their resonances at the highest field (between –310 and –340 ppm). For the diaminated tetrazolium (**6** and **7**) and triazolium (**8** and **9**) salts, the two amino group resonances (three in the case of the triazolium salts) can be differentiated by the larger inductive effect of nitrogen over carbon, which shifts the $N–NH_2$ group resonances to lower field than the $C–NH_2$ resonances. Finally, for the tetrazolium salts, N-1 and N-4 resonate in the middle of the negative region between ca. –110 and ca. –190 ppm, and can be distinguished by the larger PIS/MIS effect on the methylated nitrogen atom (i.e., more negative shift). In **9**, the three amino groups (N-4, N-5 and N-6) have very similar resonances between –322 and –335 ppm, comparable to the remainder of the compounds. The amino group-bound nitrogen atom (N-3) has a shift very similar to that of the methylated nitrogen atom (N-1) at ca. –239 ppm and more negative than that of the other triazole ring nitrogen atom (N-2, δ = –163.8 ppm). This is in contrast to **8**, in which the PIS effect on N-1 is smaller than the MIS on N-1 in **9** and the two signals have distinctive resonances (for N-1: –177.1 and N-3: –338.9 ppm). Lastly, for all compounds the observed coupling constants at two and three bonds (^{2}J and ^{3}J) have values that in general are in the range between 1.5 and 2.5 Hz, whereas those to the amino group protons are much larger (^{1}J ca. 80–90 Hz). A summary of the coupling constants is also given in Table 1. These coupling constants are in good agreement with typical values for ^{1}J, ^{2}J and $^{3}J(^{1}H,^{15}N)$.[27]

Molecular Structures

Crystals of the azolium picrate salts were obtained by slow cooling of concentrated solutions of the compounds in hot water. Recrystallization of **3** from several solvents

Table 2. Structure solution and refinement for azolium picrate salts.[a]

Parameter	**2**	**4**	**5**	**8**	**9**
Empirical formula	$C_8H_8N_8O_7$	$C_9H_{10}N_8O_7$	$C_9H_{10}N_8O_7$	$C_8H_9N_9O_7$	$C_9H_{11}N_9O_7$
Formula weight [g mol^{-1}]	328.22	342.25	342.25	343.214	357.27
Temperature [K]	200(2)	200(2)	100(2)	200(2)	100(2)
Crystal size [mm]	0.35 × 0.25 × 0.20	0.35 × 0.25 × 0.20	0.30 × 0.15 × 0.04	0.35 × 0.25 × 0.03	0.20 × 0.05 × 0.05
Crystal system	triclinic	monoclinic	monoclinic	triclinic	monoclinic
Space group	$P\bar{1}$	$P2_1/c$	$P2_1/c$	$P\bar{1}$	$P2_1/c$
a [Å]	5.895(1)	14.862(1)	14.6340(4)	3.789(1)	13.030(1)
b [Å]	10.126(1)	5.7352(4)	5.9538(2)	12.833(1)	3.8299(2)
c [Å]	11.578(1)	16.839(1)	16.3299(4)	13.935(1)	28.5923(2)
α [°]	106.96(1)	90.00	90.00	103.78(1)	90.00
β [°]	100.88(1)	104.96(1)	102.396(3)	90.38(1)	99.184(5)
γ [°]	98.02(1)	90.00	90.00	96.94(1)	90.00
V_{UC} [Å^3]	635.1(1)	1386.7(2)	1389.62(7)	652.84(1)	1408.5(1)
Z	2	4	4	2	4
ρ_{calc} [g cm^{-3}]	1.716	1.639	1.636	1.746	1.685
μ [mm^{-1}]	0.152	0.143	0.142	0.154	0.146
$F(000)$	336	704	704	352	736
θ range [°]	4.16–30.06	3.91–30.07	3.65–26.00	3.93–29.99	3.69–27.00
Index ranges	±8, ±14, ±16	±8, ±20, ±23	±18, ±7, ±20	±4, ±15, ±17	±16, ±4, ±36
Reflections collected	8662	17842	13086	6632	13091
Independent reflections	3712	4058	2724	2560	3050
Data/restraints/parameters	3712/0/240	4058/0/257	2724/0/257	2560/0/253	3050/0/270
Goodness-of-fit on F^2	1.110	1.180	1.114	1.083	1.056
R_1 [$F > 4\sigma(F)$]	0.0437	0.0649	0.0445	0.0542	0.0539
R_1 (all data)	0.0577	0.0951	0.0780	0.0671	0.0919
wR_2 [$F > 4\sigma(F)$]	0.1192	0.1303	0.0800	0.1445	0.1187
wR_2 (all data)	0.1302	0.1475	0.0941	0.1581	0.1210

[a] $R_1 = \Sigma \, ||F_o| - |F_c|| / \Sigma \, |F_o|$. $R_w = [\Sigma \, (F_o^2 - F_c^2) / \Sigma \, w \, (F_o)^2]^{1/2}$. $w = [\sigma_c^2 \, (F_o^2) + (xP)^2 + yP]^{-1}$, $P = (F_o^2 - 2F_c^2)/3$.

(e.g., alcohol, water or acetone) resulted in all cases in the recovery of the powdery compound, whereas **7** forms as a microcrystalline solid (after recrystallization from water) with bad quality (i.e., not measurable) crystals. Therefore any diffraction analysis of these two compounds was omitted. The X-ray crystallographic data for **2** and **4** were collected with an Enraf–Nonius Kappa CCD diffractometer. Data sets for **5**, **8** and **9** were collected with an Oxford Diffraction Xcalibur 3 diffractometer fitted with a CCD detector.[28] All data were collected by use of graphite-monochromated Mo-K_α radiation (λ = 0.71073 Å). No absorption corrections were applied to data sets collected for any of the compounds. All structures were solved by direct methods (SHELXS-97 and SIR97)[29,30] and refined by means of full-matrix, least-squares procedures by use of SHELXL-97. All non-hydrogen atoms were refined anisotropically. For all compounds, all hydrogen atoms were located from difference Fourier electron density maps and refined isotropically. Crystallographic data are summarized in Table 2, selected bond lengths and angles are reported in Table 3, and hydrogen-bonding geometries in Table 4. The Supporting Information contains the tabulated results of the graph-set analysis (Table S1, Table S2, Table S3 and Table S4).

Table 3. Selected bond lengths and angles in the azolium cations of picrate salts.[a]

Distances [Å]	**2**	**4**	**5**	**8**	**9**
B–N	1.316(2)	1.315(2)	1.324(3)	1.394(3)	1.407(3)
B–A_1	1.336(1)	1.337(2)	1.356(3)	1.355(3)	1.382(3)
B–A_2	1.366(1)	1.371(2)	1.339(3)	1.387(3)	1.353(3)
A_1–R_1	1.452(2)	1.459(3)	1.461(3)	1.322(3)	1.345(4)
A_1–N	1.357(2)	1.364(2)	1.337(2)	1.326(3)	1.311(3)
N–N	1.271(2)	1.273(3)	1.289(2)	1.400(2)	1.408(3)
N–R_3			1.463(3)		1.450(3)
N–A_2	1.335(2)	1.340(2)	1.340(2)	1.305(3)	1.316(3)
A_2–R_2		1.458(3)		1.357(3)	1.323(4)
Angles [°]					
N–B–A_1	128.1(1)	127.9(2)	124.8(2)	122.5(2)	131.4(2)
N–B–A_2	127.1(1)	127.3(2)	126.6(2)	130.1(2)	121.0(2)
A_2–B–A_1	104.6(1)	104.8(2)	108.6(2)	107.3(2)	107.6(2)
B–A_1–R_1	128.9(1)	128.8(2)	128.9(2)	125.2(2)	122.8(3)
N–A_1–R_1	121.7(1)	121.2(2)	121.1(2)	128.9(2)	126.6(3)
B–A_1–N	109.4(1)	109.5(2)	109.9(2)	106.0(2)	110.5(2)
A_1–N–N	107.9(1)	107.8(2)	102.7(2)	111.8(2)	104.1(2)
N–N–R_3			121.2(2)		119.1(2)
R_3–N–A_2			122.2(2)		128.7(2)
N–A_2–R_2		121.7(2)		126.9(2)	128.7(3)
N–A_2–B	109.8(1)	109.5(2)	102.1(2)	110.9(2)	106.5(2)
N–N–A_2	108.1(1)	108.2(2)	116.6(2)	104.0(2)	111.3(2)
B–A_2–R_2		128.6(2)		122.1(2)	124.8(3)

[a] 2: B = C1, A_1 = N2, A_2 = N5, R_1 = C2; 4: B = C1, A_1 = N2, A_2 = N5, R_1 = C2, R_2 = C3; 5: B = C1, A_1 = N2, A_2 = N5, R_1 = C2, R_3 = C3; 8: B = N4, A_1 = C3, A_2 = C4, R_1 = N3, R_2 = N5. 9: B = N2, A_1 = C3, A_2 = C1, R_1 = N6, R_2 = N3, R_3 = C2.

CCDC-694277 (for **4**), -694278 (for **5**), -644039 (for **8**) and -650723 (for **9**) contain the supplementary crystallographic data for this paper. This data can be obtained free of charge from The Cambridge Crystallographic Data Centre via www.ccdc.cam.ac.uk/data_request/cif.

Table 4. Selected hydrogen bonds for azolium picrate salts (distances in Å, angles in °).[a]

D–H···A	D–H	H···A	D–H···A	D–H–A
		2[(a)]		
N1–H1A···O2^{i}	0.92(2)	2.14(2)	3.035(2)	163(2)
N1–H1B···O1^{ii}	0.88(2)	2.35(2)	3.019(2)	132(2)
N1–H1B···O2^{ii}	0.88(2)	2.52(2)	3.199(2)	134(2)
N5–H5···O1^{ii}	0.94(2)	1.82(2)	2.618(1)	134(2)
N5–H5···O7^{ii}	0.94(2)	2.16(2)	2.896(2)	140(2)
		4[(b)]		
N1–H1A···O1	1.00(2)	1.76(2)	2.747(2)	170(2)
N1–H1A···O2	1.00(2)	2.45(2)	2.970(2)	112(1)
N1–H1B···O3^{i}	0.87(3)	2.05(3)	2.894(2)	163(2)
		5[(c)]		
N1–H1A···O3^{i}	0.90(3)	2.20(3)	3.019(3)	151(2)
N1–H1B···O1^{ii}	0.88(3)	1.95(3)	2.686(2)	140(2)
		8[(d)]		
N1–H5···O4	0.86(3)	2.57(3)	3.157(3)	126(3)
N3–H1···N1	0.88(3)	2.49(3)	2.867(3)	107(2)
N3–H1···O7^{ii}	0.89(3)	2.24(3)	3.072(3)	154(2)
N4–H7···O1^{ii}	0.90(3)	1.92(3)	2.653(2)	137(2)
N4–H7···O2^{ii}	0.90(3)	2.25(3)	3.014(2)	142(2)
N5–H3···N6^{ii}	0.90(3)	2.12(3)	2.993(3)	162(3)
N1–H6···O5^{iii}	0.86(3)	2.26(3)	3.034(3)	150(2)
N3–H1···O6^{iv}	0.88(3)	2.27(3)	3.136(3)	168(3)
		9[(e)]		
N3–H3A···N1	0.80(3)	2.52(3)	2.834(4)	105(2)
N3–H3A···O3	0.80(3)	2.26(3)	2.779(3)	123(3)
N3–H3B···O5^{i}	0.89(4)	2.15(4)	3.018(4)	165(3)
N6–H6A···O1^{ii}	0.86(4)	2.11(4)	2.944(3)	163(3)
N6–H6A···O7^{ii}	0.86(4)	2.56(4)	3.118(3)	124(3)
N1–H1B···O1^{ii}	0.84(4)	2.12(4)	2.924(4)	160(3)
N1–H1B···O2^{ii}	0.84(4)	2.34(3)	2.834(4)	118(3)
N6–H6B···N5^{iii}	0.93(4)	2.18(4)	3.062(4)	158(3)

[a] Symmetry codes: [(a)] (i) 1 + x, 1+ y, z; (ii) –x, 1 – y, 2 – z. [(b)] (i) 1 – x, 0.5 + y, 0.5 – z. [(c)] (i) 1 – x, 2 – y, – z; (ii) x, 2.5 – y, 0.5 + z. [(d)] (ii) 1 + x, y, 1 + z; (iii) 1 + x, y, z; (iv) 2 – x, –y, 1 – z. [(e)] (i) 1 – x, 0.5 + y, 0.5 – z; (ii) 1 – x, 2 – y, 1 – z; (iii) 2 – x, 4 – y, 1 –z.

The crystal structure of **2** was reported during the course of our research on azolium picrate salts,[20b] so only the features in the structure not described before are highlighted (i.e., graph-sets). The rest of the picrate salts have been crystallographically characterized for the first time in this work and a detailed description of their molecular structures and packing follows. Since the picrate anion is well established, its structure is not discussed in detail here.

Among the picrate salts studied here, **2** and **8** are the only ones that crystallize in triclinic cells in the space group $P\bar{1}$, whereas the rest of the compounds have monoclinic cells in the space group $P2_1/c$. In the structure of **2**, polymeric chains are formed along the a axis with simple van der Waals interactions between chains. Although cations and anions do not pack in a layered structure (Figure 5), coplanarity exists between cations and anions. Since the performance of a material is a function (among other properties) of its density and this is governed by the molecular structure and hydrogen bonding, it is of interest to take a closer look at the hydrogen-bonding motifs formed in the

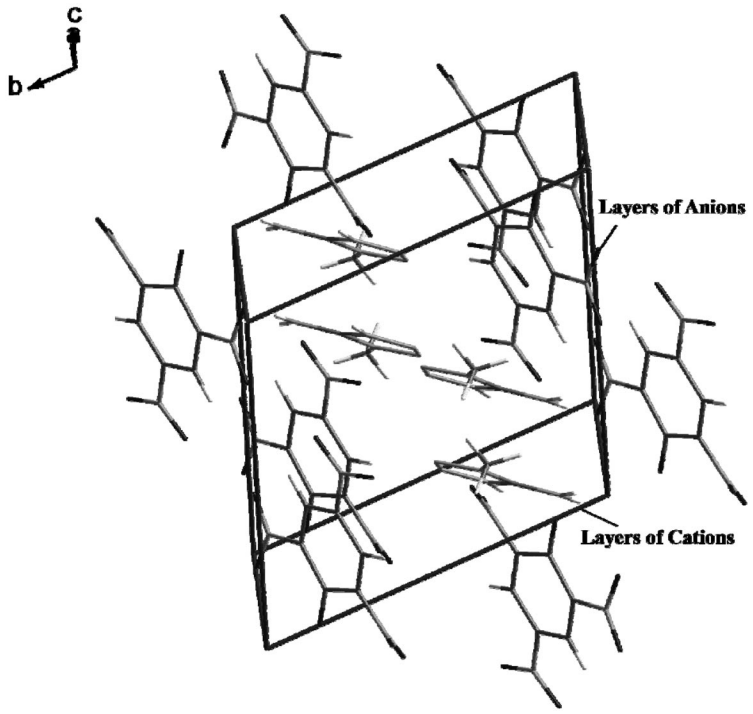

Figure 5. Layers of cations and anions in the unit cell of **2** (view along the *a* axis).

crystal structure. The formalism of graph-set introduced by Bernstein et al.[31] and the program *RPLUTO*[32] are useful for assigning and describing patterns in the hydrogen bonding. The five hydrogen bonds tabulated in Table 4 could be identified by the program as forming common finite interactions of the type D1,1(2) at the primary level (see Supporting Information Table S1). These dimeric interactions combine at the secondary level to form exclusively ring graph-sets of variable sizes going from the small R2,2(4) to the large R4,4(26) graph sets. Some of the most characteristic patterns are depicted in Figure 6. For example, the phenolate oxygen atom interacts (together with one of the *o*-NO_2 oxygen atoms) with two of the cation hydrogen atoms to form one very strong [N5···O1^{ii} 2.618(1) Å] and three medium [N1···O1^{ii}, N1···O2^{ii} and N5···O7^{ii} 2.9–3.2 Å; symmetry code: (ii) –*x*, 1 – *y*, 2 – *z*] hydrogen bonds, which describe two R2,1(6) motifs. A similar pattern is also formed by the cation; in this case it enters into two interactions through two different hydrogen atoms and thus takes the label R1,2(6). Lastly, two symmetrically generated cations and anions are linked together through interaction with the amino group protons, yielding a larger R2,4(8) ring graph-set. This is identical to the patterns found in compounds containing the 14DMAT$^+$ cation and analogous to the R4,4(12) motif found in the perchlorate salt.[18c]

Unlike in **2**, in which the amino group protons are approximately coplanar to the tetrazole ring, in the structure of **4** these are bent out of the plane [H1B–N1–C1–N2 165(1)°]. The formal exchange of a proton in **2** for a methyl group in **4** results in a less efficient packing, as represented in Figure 7 and reflected in a decrease in the density from 1.716 to 1.639 g cm^{-3}. In addition, fewer hydrogen bonds are formed (**5** vs. **3**).

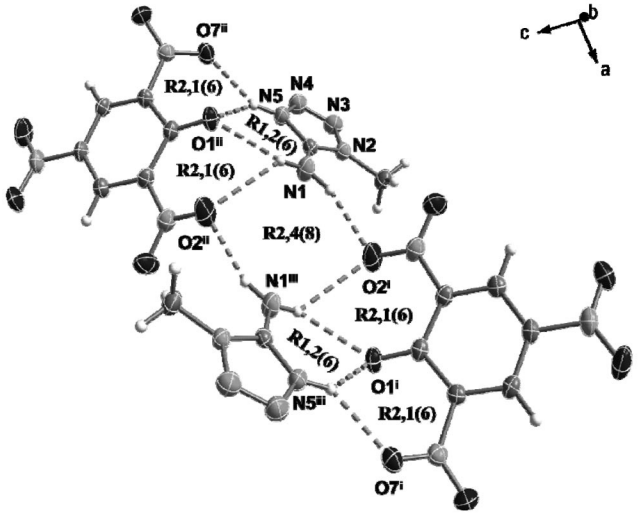

Figure 6. Hydrogen bonding in the crystal structure of picrate salt **2** showing some characteristic ring graph-sets [symmetry codes: (i) 1 + *x*, 1 + *y*, *z*; (ii) –*x*, 1 – *y*, 2 – *z*; (iii) 1 – *x*, 2 – *y*, 2 – *z*].

Once again, the phenolate anion participates in the formation of an R2,1(6) graph-set and the N5-bound methyl group forms a nonclassical hydrogen bond to O7 [C3···O7 3.401(3) Å]. As can be seen in Figure 8, the orientation of the ions does not allow the formation of the R2,4(8) pattern mentioned above for **2**, but one of the cations interacts through N1 with two picrate anions [N1···O1 2.747(2) and N1···O3^i 2.894(2) Å; symmetry code: (i) 1 – *x*, 0.5 + *y*, 0.5 – *z*], which in turn form a hydrogen bond to two crystallographically related cations [N1^i and N1^{ii}; symmetry code: (ii) 1 – *x*, –0.5 + *y*, 0.5 – *z*]. This is in contrast with the

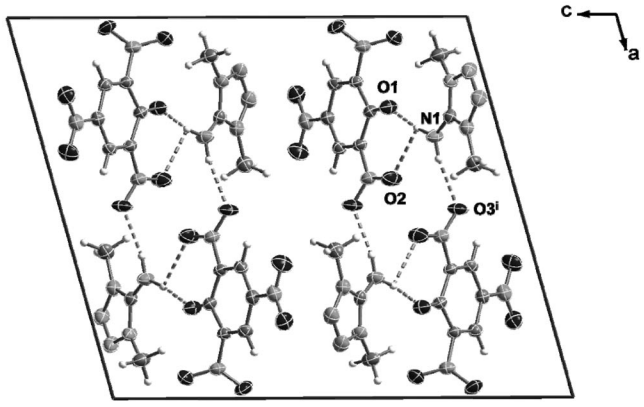

Figure 7. View of the unit cell of picrate salt **4** along the *b* axis, showing the hydrogen bonding [dotted lines, symmetry code: (i) 1 – *x*, 0.5 + *y*, 0.5 – *z*].

iodide,[54] azide and perchlorate salts and is analogous to the dinitramide compound.[18c] Lastly, two chain graph-sets of the type C2,2(X) (X = 6, 8) are found at the secondary level (Supporting Information Table S2).

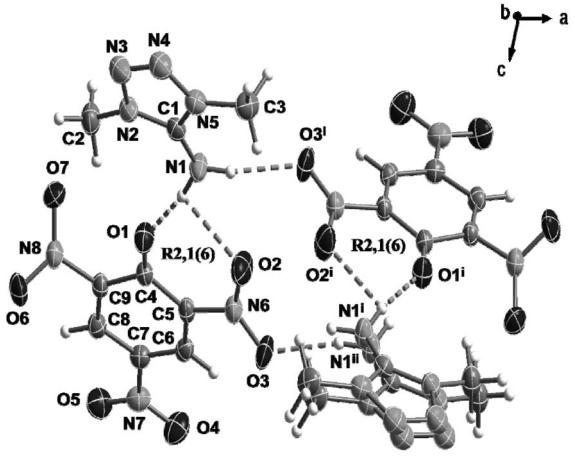

Figure 8. Hydrogen bonding in the crystal structure of **4** showing some characteristic ring graph-sets [symmetry codes: (i) 1 –*x*, 0.5 + *y*, 0.5 – *z*; (ii) 1 – *x*, –0.5 + *y*, 0.5 – *z*].

Compound **5** (Figure 9) is the "asymmetric" isomer of **4**. Both compounds crystallize in the same monoclinic space group ($P2_1/c$) and have very similar cell parameters (Table 2) and almost identical unit cell volumes (ca. 1390 Å^3). Views along the *b*-axes of the unit cells of **4** (Figure 7) and **5** (Figure 10) make the similarities in the structures of the two compounds obvious. Only one medium hydrogen bond [N1···O3^i 3.019(3) Å] and one strong hydrogen bond [N1···O1^{ii} 2.686(2) Å] are formed [symmetry codes: (i) 1 – *x*, 2 – *y*, –z; (ii) *x*, 2.5 – *y*, 0.5 + *z*]. As in **4**, two cations and two anions are connected through hydrogen bonds (Table 4) and again the two picrate anions are linked once to the same cation and once to two crystallographically related cations.

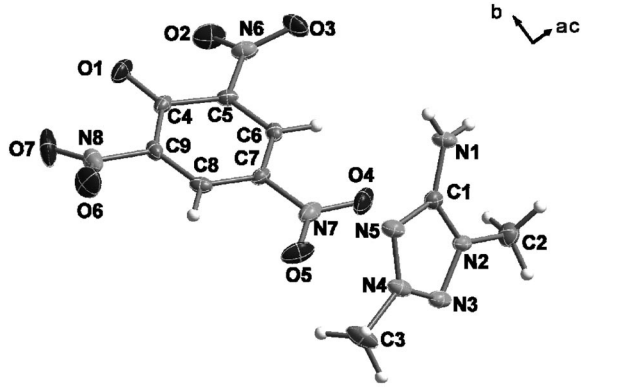

Figure 9. Asymmetric unit of picrate salt **5** with the labelling scheme.

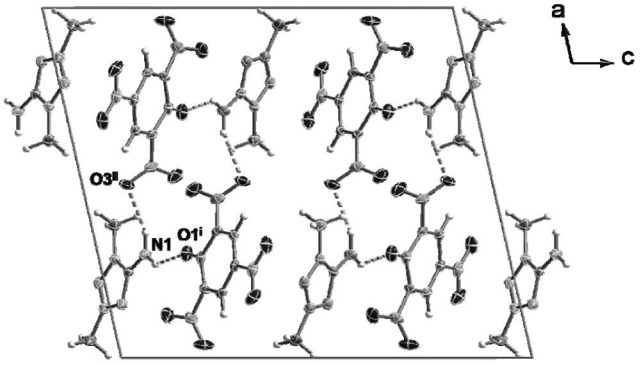

Figure 10. View of the unit cell of picrate salt **5** along the *b* axis showing the hydrogen bonding [dotted lines, symmetry codes: (i) 1 – *x*, 2 – *y*, –z; (ii) *x*, 2.5 – *y*, 0.5 + *z*].

In **5**, the arrangement of the anions does not allow the formation of the R2,1(6) graph-set described for **4**, and only a chain C2,2(8) motif involving both hydrogen bonds is found (Supporting Information Table S3) instead of the expected R2,2(16) pattern that would form if the interacting cations and anions were to lie in the same plane. This lack of efficiency in the packing is reflected in the lower density values (ca. 1.64 g cm^{-3}) of both compounds with respect to the other salts reported here.

In **9** the picrate anion shows two essentially planar nitro groups whereas the third one is clearly out of the plane formed by the aromatic ring with a torsion angle (C4–C9–N9–O7) of ca. –38°. It is precisely this out-of-plane nitro group that participates in the formation of a nonclassical hydrogen bond with the methyl group in the methylguanazinium cation [C2···O7^{iv} 3.259(4) Å; symmetry code: (iv) 1 + *x*, 1 + *y*, *z*] with H1···O7^{iv} 2.54(5) Å (sum of the van der Waals radii $r_O + r_H$ = 2.70 Å),[33] as already observed for other picrate salts.[20a] As shown in Figure 11, cations and anions alternate along the *c* axis, whereas there exist π-stacks of anions and cations along the *b* axis connected by extensive hydrogen-bonding. The presence of three amino groups in the cation is reflected in the larger number of hydrogen bonds formed in relation to the other picrate salts described in this report (Table 4).

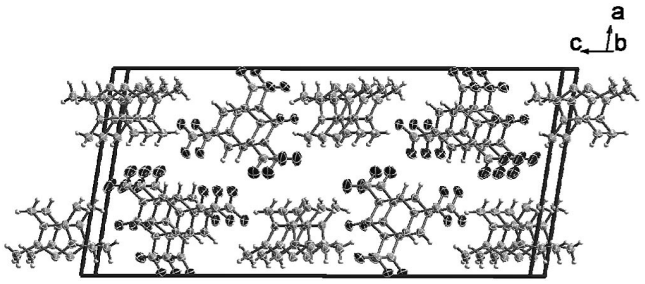

Figure 11. View of the unit cell of picrate salt **9** showing the stacks of cations and anions along the *b* axis.

In addition to the non-classical C···O hydrogen bond, every cation is involved in the formation of eight other hydrogen bonds (Figure 12), two of which are to another cation, yielding an R2,2(8) subset at the primary level [N6···N5^{iii} 3.062(4) Å; symmetry code: (iii) 2 – *x*, 4 – *y*, 1 – *z*]. Also at the primary level, an S(5) motif [N3···N1 2.834(4) Å] is found, analogously with **8**[59a] and common to other 1,2-diaminosubstituted azoles.[18d,58,34] The rest of the hydrogen bonds are to three crystallographically related anions. It is interesting to note that one of these anions alone forms up to four different medium-to-strong hydrogen bonds to the same triazolium cation [N1···O1^{ii} 2.924(4), N1···O2^{ii} 2.834(4), N6···O1^{ii} 2.944(3) and N6···O7^{ii} 3.118(3) Å; symmetry code: (ii) 1 – *x*, 2 – *y*, 1 – *z*], describing two R2,1(6) subsets (similarly to 2) and one R1,2(7) motif through interaction of the phenolate oxygen atom (O1^{ii}), N1 and N6 at the same time. Lastly, apart from the graph-set described above there exist (among others) many large ring patterns of the type R4,4(X) (X = 18, 22, 24, 28) and infinite hydrogen-bonded chains, which take the label C2,2(X) (X = 10, 13, 14, 15) (see Supporting Information Table S4).

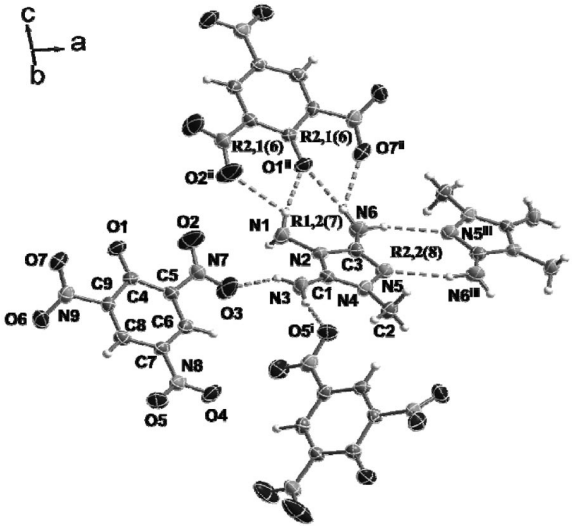

Figure 12. Hydrogen bonding in the crystal structure of **9** showing some characteristic ring graph-sets [symmetry codes: (i) 1 – *x*, 0.5 + *y*, 0.5 – *z*; (ii) 1 –*x*, 2 –*y*, 1 –*z*; (iii) 2 –*x*, 4 – *y*, 1 – *z*].

Energetic Properties

Computational Methods

All quantum chemical calculations were carried out by use of the Gaussian03W software package.[35] Electronic energies for all cations and the picrate anion were calculated by Møller–Plesset perturbation theory truncated at the second-order (MP2)[36] and were used unscaled (Supporting Information Table S5). The structures of the cations and anion were optimized from the single-crystal structures by use of the correlation consistent polarized double-zeta basis set cc-pVDZ.[37] All of the optimized structures were characterized to be true minima on the potential energy surface without imaginary frequencies.

The heat of formation ($\Delta H°_f$) of an ionic salt can be calculated from the heats of formation of cation and anion and the lattice energy (ΔH_L) by Born–Haber energy cycles[38] through Equation (1). The lattice energy can, in turn, be calculated by application of Jenkins' Equation [Equation (2)][39] from the lattice potential energy (U_{POT}) and n_x and n_y, which are indexes for the ions X_a^+ and Y_b^-, and are equal to 3 for monoatomic ions, 5 for polyatomic ions and 6 for nonlinear polyatomic ions. Lastly, the lattice potential energies can readily be derived from the density of the material (ρ) in g cm^{-3}, the chemical formula mass (M) in g, and the coefficients γ (kJ mol^{-1} cm^{-1}) and δ (kJ mol^{-1}) that take their values from the literature[39] according to Equation (3).

$$\Delta H°_f \text{ (ionic salt, 25 °C)} = \Delta H°_f \text{ (cation, 25 °C)} + \Delta H°_f \text{ (anion, 25 °C)} - \Delta H_L \quad (1)$$

$$\Delta H_L = U_{POT} + [a(n_x/2 - 2) + b(n_y/2 - 2)]RT \quad (2)$$

$$U_{POT} = \gamma\,(\delta/M)^{1/3} + \delta \quad (3)$$

In order to assess the energetic properties of the azolium picrate salts, the thermal stability (DSC measurements) and sensitivity to friction, impact, electrostatic discharge and thermal shock of each salt was experimentally determined. For each salt the constant volume energy of combustion was determined experimentally by oxygen bomb calorimetry and was also predicted on the basis of calculated electronic energies (see Computational Methods section above and Supporting Information Table S5) and an estimation of lattice enthalpy.[39,40] Prediction of thermochemical properties of energetic materials by similar methods has been described before.[41] The energies of formation were calculated from the experimentally measured combustion data and used in conjunction with the calculated (from the X-ray measurements) or experimentally determined (from picnometer measurements) densities and the molecular formulas to calculate the detonation pressures and velocities with the aid of the EXPLO5 computer code.[42]

DSC measurements on a small sample of each salt in this study show distinctive melting points for the methylated derivatives (**2**–**5** and **9**) between 175 and 210 °C (Table 5), well apart from their decomposition temperatures (all of them above 250 °C). Compound **2** melts at 175 °C, whereas the

replacement of one of the protons in the compound by a methyl group in **4** results in an increase of the melting point to 210 °C, as also observed for other salts with the $1MAT^+$ and $14DMAT^+$ cations.[18c] Compound **9** shows a defined melting point at 207 °C, which is in contrast with nonmethylated guanazinium salts, which generally melt with concomitant decomposition,[57,58,59a] whereas the isomer of **4** (**5**), as would be expected because of the asymmetric substitution pattern that makes the packing in the solid state less effective, has a lower melting point similar to that of the monomethylated picrate salt **2** (T_m = 180 °C). All compounds have excellent (very similar) thermal stabilities above 250 °C. The liquid ranges (differences between melting and decomposition points) of **2**, **4**, **9** and **5** are ca. 95, ca. 59, ca. 43 and ca. 98 °C, respectively, making **2** and **5** of prospective interest as new energetic compounds for use in melt-casting explosives. On the other hand, the nonmethylated compounds (**1**, **6** and **8**) either have narrow liquid ranges (e.g., **1**: ca. 30 °C) or melt with concomitant decomposition. Apart from **1** and **6**, which decompose slowly at temperatures above 170 °C, the rest of the materials have excellent thermal stabilities to temperatures as high as 278 °C (**5**). The trend in the decomposition (and melting) points is, in general, to increase with the number of carbon atoms; however, the guanazinium salts with three amino groups readily enter into extensive hydrogen bonding (see X-ray discussion), which increases thermal stability. In comparison with commonly used high explosives, the azolium picrate salts discussed here have melting points that are as a rule between that of TNT (81 °C) and that of RDX (204 °C),[15] whereas the decomposition points are generally comparable to that of RDX (230 °C). In addition to DSC analysis, the response of the compound to fast heating in the flame of a Bunsen burner was also tested. In all cases the picrate salts burned nicely with little smoke, and in the case of the more energetic $5At^+$, DAT^+ and Gz^+ salts the compounds burned markedly more rapidly, as might be expected from the higher detonation parameters of the compounds (see discussion below). This is a response similar to that observed in high explosives such as TNT or picric acid. From these "flame test" observations it would seem that the azolium picrates containing higher percentages of nitrogen are more sensitive to thermal shock.

Data collected for friction, impact and electrostatic discharge sensitivity testing are summarized in Table 6. None of the compounds exploded under the drop hammer (impact sensitivity >40 J) and they were also not sensitive towards friction at the maximum setting of a BAM tester (friction sensitivity >360 N).[44–46] These observations are interesting since picric acid itself is more sensitive to both impact and friction[15] and puts into perspective the potential of azolim picrate salts as insensitive energetic materials regardless of their higher (less negative) heats of formation in relation to picric acid. Additionally, each salt was also roughly tested for sensitivity to electrostatic discharge by spraying of sparks across a small sample of the material with the aid of a Tesla coil (electrostatic discharge from an HF-Vacuum-Tester type VP 24). None of the compounds turned out to be sensitive to an electrostatic discharge of ca. 20 kV, similarly to TNT.[47] Lastly, all of the compounds in this study can be classified as insensitive according to the UN Recommendations on the Transport of Dangerous Goods as described in ref.[44]

Apart from sensitivity issues, the performance of energetic materials is also of critical importance. The EXPLO5 computer code[42] can be used to predict the performance of CHNO-based energetic compounds. Therefore, the energies of formation of the azolium picrate salts in this study were back-calculated from their heats of combustion on the basis of their combustion equations (see below) by applica-

Table 5. Physico-chemical properties of azolium picrate salts.

	1	**2**	**3**	**4**	**5**	**6**	**7**	**8**	**9**
Formula	$C_7H_6N_8O_7$	$C_8H_8N_8O_7$	$C_8H_8N_8O_7$	$C_9H_{10}N_8O_7$	$C_9H_{10}N_8O_7$	$C_7H_7N_9O_7$	$C_8H_9N_9O_7$	$C_8H_9N_9O_7$	$C_9H_{11}N_9O_7$
Mol. mass [g mol^{-1}]	314.17	328.05	328.05	342.25	342.25	329.19	343.21	343.20	357.24
T_m [°C][a]	148	175	161	210	180	170	148	–	207
T_d [°C][b]	>175	270	242	269	278	174	154	269	250
N (%)[c]	35.7	34.1	34.1	32.7	32.7	38.3	36.7	36.7	35.3
$N + O$ (%)[d]	71.3	68.3	68.3	65.5	65.4	72.3	69.3	69.3	66.6
Ω (%)[e]	–50.9	–63.4	–63.4	–74.8	–74.8	–51.0	–62.9	–62.9	–73.9
ρ [g cm^3][f]	1.840	1.716	1.711[k]	1.639	1.636	1.756	1.688[k]	1.746	1.685
$\Delta_c U$ [cal g^{-1}][g,j]	–2650(10) [–2899]	–3000(35) [–3251]	–2990(20) [–3236]	–3320(30) [–3572]	–3310(25) [–3558]	–2780(10) [–2936]	–3100(10) [–3267]	–3000(30) [–3179]	–3310(15) [–3486]
$\Delta U°_f$ [kJ kg^{-1}] [h,j]	–320(30) [718]	–440(145) [609]	–460(80) [549]	–540(130) [506]	–580(100) [448]	330(50) [962]	160(40) [838]	–250(130) [470]	–370(60) [369]
$\Delta H°_f$ [kJ kg^{-1}] [i,j]	–410(30) [635]	–520(145) [522]	–550(80) [463]	–630(130) [416]	–670(100) [357]	240(50) [875]	65(40) [748]	–350(130) [380]	–470(60) [276]

[a] Chemical melting point and [b] decomposition point (DSC onsets) from measurement with β = 5 °C min^{-1}. [c] Nitrogen percentage. [d] Combined nitrogen and oxygen percentages. [e] Oxygen balance according to ref.[43]. [f] Density from X-ray measurements. [g] Calculated constant pressure heat of combustion. [h] Standard heat of formation (back-calculated from $\Delta H_{comb.}$). [i] Standard heat of formation. [j] Uncertainties are given in parentheses, calculated values (from MP2 electronic energies) are given in square brackets. [k] Experimentally determined density from picnometer measurements.

Table 6. Initial safety testing results and predicted and calculated[a] energetic performances of azolium picrate salts by use of the EXPLO5 code.

	T_{ex} [K][b]	V_0 [L kg^{-1}][c]	P [GPa][d]	D [m s^{-1}][e]	Impact [J][f]	Friction (N)[f]	ESD (+/–)[g]	Thermal shock
1	3395 [3978]	665 [674]	25.6 [30.1]	7795 [8308]	>40	>360	–	burns rapidly
2	3205 [3745]	672 [681]	21.2 [24.5]	7343 [7755]	>40	>360	–	burns
3	3168 [3718]	672 [681]	20.4 [24.2]	7213 [7722]	>40	>360	–	burns
4	3005 [3555]	675 [682]	17.8 [21.2]	6876 [7384]	>40	>360	–	burns
5	2986 [3501]	674 [682]	17.6 [20.4]	6846 [7252]	>40	>360	–	burns
6	3663 [4011]	694 [699]	25.4 [27.8]	7864 [8143]	>40	>360	–	burns rapidly
7	3429 [3755]	694 [700]	22.1 [23.7]	7492 [7682]	>40	>360	–	burns
8	3201 [3580]	688 [693]	22.5 [25.0]	7495 [7808]	>40	>360	–	burns rapidly
9	3029 [3403]	688 [693]	19.8 [22.1]	7162 [7486]	>40	>360	–	burns

[a] Calculated values in square [ ] brackets. [b] Temperature of the explosion gases. [c] Volume of the explosion gases. [d] Detonation pressure. [e] Detonation velocity. [f] Tests by BAM methods (see refs.[44–46]). [g] Rough sensitivity to 20 kV electrostatic discharge (ESD); + sensitive, – insensitive from an HF-Vacuum-Tester type VP 24.

tion of Hess's Law and the known standard heats of formation for water and carbon dioxide[48] and a correction for change in gas volume during combustion. No corrections for the non-ideal formation of nitric acid (typically ca. 5% of the nitrogen content reacts to form HNO_3) were made. This is justified by the relatively large standard deviation from the combustion measurements. The EXPLO5 code was used, with the following values for the empirical constants in the Becker–Kistiakowsky–Wilson equation of state (BKWN-EOS): $\alpha = 0.5$, $\beta = 0.176$, $\kappa = 14.71$ and $\theta = 6620$. Because of the reasonably large standard deviations of experimental combustion measurements, the enthalpies of combustion for each material were predicted on the basis of published methods, with use of calculated electronic energies and an approximation of lattice enthalpy,[39,40] in order to validate the experimentally determined values.

Compound **1**: $[CH_4N_5]^+$ $[C_6H_2N_3O_7]$ (s) + 5 O_2 → 7 CO_2 (g) + 3 H_2O (l) + 4 N_2 (g)

Compound **2**: $[C_2H_6N_5]^+$ $[C_6H_2N_3O_7]$ (s) + 6.5 O_2 → 8 CO_2 (g) + 4 H_2O (l) + 4 N_2 (g)

Compound **3**: $[C_2H_6N_5]^+$ $[C_6H_2N_3O_7]$ (s) + 6.5 O_2 → 8 CO_2 (g) + 4 H_2O (l) + 4 N_2 (g)

Compound **4**: $[C_3H_8N_5]^+$ $[C_6H_2N_3O_7]$ (s) + 8 O_2 → 9 CO_2 (g) + 5 H_2O (l) + 4 N_2 (g)

Compound **5**: $[C_3H_8N_5]^+$ $[C_6H_2N_3O_7]$ (s) + 8 O_2 → 9 CO_2 (g) + 5 H_2O (l) + 4 N_2 (g)

Compound **6**: $[CH_5N_6]^+$ $[C_6H_2N_3O_7]$ (s) + 5.25 O_2 → 7 CO_2 (g) + 3.5 H_2O (l) + 4.5 N_2 (g)

Compound **7**: $[C_2H_7N_6]^+$ $[C_6H_2N_3O_7]$ (s) + 6.75 O_2 → 8 CO_2 (g) + 4.5 H_2O (l) + 4.5 N_2 (g)

Compound **8**: $[C_2H_7N_6]^+$ $[C_6H_2N_3O_7]$ (s) + 6.75 O_2 → 8 CO_2 (g) + 4.5 H_2O (l) + 4.5 N_2 (g)

Compound **9**: $[C_3H_9N_6]^+$ $[C_6H_2N_3O_7]$ (s) + 8.25 O_2 → 9 CO_2 (g) + 5.5 H_2O (l) + 4.5 N_2 (g)

The experimentally determined constant volume energies of combustion [$\Delta_c U_{(exp)}$] of all azolium picrate salts were determined by oxygen bomb calorimetry to be –2650(10) cal g^{-1} (**1**), –3000(35) cal g^{-1} (**2**), –2990(20) cal g^{-1} (**3**), –3320(30) cal g^{-1} (**4**), –3310(25) cal g^{-1} (**5**), –2780(10) cal g^{-1} (**6**), –3125(10) cal g^{-1} (**7**), –3160(30) cal g^{-1} (**8**) and –3310(15) cal g^{-1} (**9**). If it is kept in mind that calculated values systematically tend to overestimate the experimentally determined ones, the predicted constant volume energies of combustion [$\Delta_c U_{(pred)}$] calculated by this method are in good agreement with the experimentally determined values. The overestimation in the values for the energies of formation is, in general, below 4%, in keeping with other compounds with low potential to form hydrogen bonds.[49] The largest disagreement is found (in general) for the non-methylated salts **8**, **1** and **6**, which form more hydrogen bonds and is due to the low capacity of the method to account for "strong" hydrogen bonding. Accordingly, the calculated heats (or energies) of formation have all more positive (or less negative) values than the heats of formation back-calculated from the heats of combustion. The experimentally determined values all vary all within a relatively narrow range and are slightly negative [e.g., $\Delta_c U_{(exp)}$(**5**) = –670(100) kJ g^{-1}] or slightly positive [e.g., $\Delta_c U_{(exp)}$(**6**) = +240(50) kJ kg^{-1}]. The density values vary between moderate [ρ(**5**) = 1.636 g cm^{-3}] and high [ρ(**1**) = 1.840 g cm^{-3}] and are approximately in the range of commonly used high explosives [e.g., ρ(TNT) = 1.654 g cm^{-3} or ρ(RDX) = 1.800 g cm^{-3}].

From the experimentally determined densities, chemical compositions and energies of formation (back-calculated

from the heats of combustion), the detonation pressures and velocities of **1** (7795 m s^{-1}, 25.6 GPa), **2** (7343 m s^{-1}, 21.2 GPa), **3** (7213 m s^{-1}, 20.4 GPa), **4** (6876 m s^{-1}, 17.8 GPa), **5** (6846 m s^{-1}, 17.6 GPa), **6** (7864 m s^{-1}, 25.4 GPa), **7** (7492 m s^{-1}, 22.1 GPa), **8** (7495 m s^{-1}, 22.5 GPa) and **9** (7162 m s^{-1}, 19.8 GPa) were predicted by use of the EXPLO5 code. These values are as a rule higher than those calculated for TNT (at ρ = 1.60 g cm^{-3}: 7073 m s^{-1}, 19.4 GPa) and in some instances also higher than those of picric acid itself (at ρ = 1.70 g cm^{-3}: 7185 m s^{-1}, 20.1 GPa)[15] and fit nicely with the computed ones from MP2 energies. In comparison with other azolium salts for which predicted performance data are reported, the azolium picrate salts in this study are predicted to outperform methylated aminotetrazolium salts (6200 m s^{-1}, 15.5 GPa)[54] and some of them have performances comparable to those of substituted triazolium salts (7500–7900 m s^{-1}, 20–25 GPa).[54,38,41]

A closer look into the heats of formation and detonation parameters ("experimentally determined" or computed) of the azolium picrates studied here clearly illustrates the influence of the cation in these values and allows one to draw conclusions about what sort of cations are best suited for a given application. Compound **1** has a negative heat of formation of –410(30) kJ kg^{-1}, and substitution of a proton in the ring by a methyl group as in **2** and **3** results in an increase in the exothermicity of the compounds (<–520 kJ kg^{-1}). A second methyl group as in the isomeric **4** and **5** results in further decreases in the heats of formation (<–620 kJ kg^{-1}). However, exchange of a proton in the ring of **1** for an amino group (**6**) yields an endothermic compound [+240(50) kJ kg^{-1}], and quaternization of the ring to form **7** again decreases the heat of formation [65(40) kJ kg^{-1}]. On the other hand, although triazoles are as a rule less endothermic compounds than tetrazoles (1,2,4-triazole; $\Delta_f H°_{cryst}$ = 26.1 kcal mol^{-1}) in relation to 5-*H*-tetrazole ($\Delta_f H°_{cryst}$ = 56.7 kcal mol^{-1}),[50] the three amino groups in the guanazinium salts **9** and **8** make the compounds more endothermic than the analogous tetrazolium salts with equal numbers of carbon atoms. The effect of the cation on the heats of formation is accordingly observed in the detonation parameters. The most endothermic compound (**6**) has the highest calculated values. The negative heat of formation of **1** is compensated by its high density (1.840 g cm^{-3}) and the salt has the second highest detonation velocity of the picrate salts described here, whereas the rest of the compounds have accordingly higher performances the higher their density.

All compounds have high combined oxygen and nitrogen contents (>65%) and the calculated oxygen balances range from –50 to –75%, which are comparable to those of picric acid (–43%) or TNT (–74%) and only slightly more negative than that of RDX (–22%). In view of the negative oxygen balances of the azolium picrates salts in this work, it was of interest to study the performances of mixtures of the compounds with an oxidizer. Therefore, the EXPLO5 code was used to predict the performance of mixtures of the picrate salts with ammonium nitrate (AN) and ammonium dinitramide (ADN) at an approximately neutral oxygen balance in order to increase the performance further with respect to the stand-alone compounds. The results of the calculations are summarized in the Supporting Information, Table S6 and Table S7. Formulations with AN are predicted to have highly negative heats of formation below –3200 kJ kg^{-1} but better detonation velocities than the stand-alone compounds in the 8000 to 8200 m s^{-1} range. On the other hand, mixtures with ADN as the oxidizer are predicted to have less negative heats of formation between –700 and –1100 kJ kg^{-1} and much higher detonation parameters (8700–8900 m s^{-1} and 31.0–33.0 GPa).

Lastly, it is important to point out that all performance values reported in the literature are based exclusively on heats of combustion predicted from electronic energies as discussed above. This method systematically tends to overestimate the heats of combustion, and the resulting performance values are therefore exaggerated. This overestimation is higher, the higher the possibility of a compound to enter into extensive hydrogen bonding. On the other hand, however, experimentally determined heats of formation tend to be underestimated, and performance predictions based on these should thus also be underestimated.

Decomposition Gases and Long-Term Stability

The ICT code[51] was used to predict the heats of explosion and the decomposition gases formed upon explosion/decomposition of the azolium picrate salts in this work from the experimentally determined heats of formation (back-calculated from the heats of combustion), the densities (from X-ray) and the molecular formulas. The results of the calculations are summarized in Table 7, which also contains the predicted data for TNT and PicH for comparison purposes.

As might be expected from a nitrogen-rich cation, nitrogen gas is predicted to be the major decomposition product (ca. 315–375 g kg^{-1}) for the azolium picrate salts and is expected to be formed in amounts almost twice as high as those predicted for classical nitroaromatic explosives (i.e., TNT and PicH). The amounts of carbon soot are also relatively high, due to the picrate anion, but still much lower than those formed by TNT (262 g kg^{-1}) and in the case of the nitrogen-richer **1** and **6** salts only slightly higher than those formed by PicH (ca. 182 vs. 158.5 g kg^{-1}). The major decomposition product expected from the explosion of classical nitroaromatics is anticipated to be CO_2, which is also expected to be formed in relatively large (although much smaller) amounts for **1** and **6** (269.7 and 227.7 g kg^{-1}, respectively). Water (gas) is expected to be generated in a higher ratio for the carbon-richer azolium salts and in larger amounts than for neutral nitroaromatics. In addition, only small amounts of CO are predicted by the code (20–30 g kg^{-1}) and there is expected to be little nitrogen going into the formation of NH_3 (3–13 g kg^{-1}) and negligible amounts of CH_4 (<2.1 g kg^{-1}) and highly toxic HCN (<0.4 g kg^{-1}) formed. Lastly, the heats of explosion all have

Table 7. Predicted decomposition gases and heats of explosion of azolium picrate salts and comparison with commonly used high explosives (from the ICT code).[a]

Compound	CO_2	H_2O	N_2	CO	H_2	NH_3	CH_4	HCN[b]	C	ΔH_{ex} [cal g^{-1}] [c]
1	269.7	163.1	353.4	26.7	0.2	3.7	0.2	–	182.1	1117
2	199.2	202.9	335.9	27.9	0.5	6.4	0.8	0.3	225.6	1093
3	199.1	202.8	335.9	28.1	0.5	6.5	0.8	0.3	225.5	1085
4	141.5	235.1	318.9	26.8	0.8	10.1	2.0	0.4	263.9	1066
5	141.5	234.9	318.8	26.9	0.8	10.1	2.1	0.4	263.8	1056
6	227.7	179.5	378.5	26.1	0.3	5.0	0.4	0.3	181.5	1245
7	165.2	215.5	360.3	25.6	0.6	8.3	1.0	0.3	222.9	1226
8	165.1	216.9	360.3	23.3	0.4	8.1	0.8	0.3	224.0	1265
9	113.5	245.8	342.2	21.7	0.8	12.7	1.9	0.4	260.6	1081
TNT	318.1	184.8	182.2	47.0	0.6	3.2	1.2	–	262.0	1350
PicH	495.9	113.5	182.3	47.5	0.2	1.1	0.2	–	158.5	1272

[a] The amount of gases formed at 298 K is given in grams of gas per kilogram of energetic compound. [b] No HCN formation was predicted for **1**, TNT and PicH. [c] Heat of explosion.

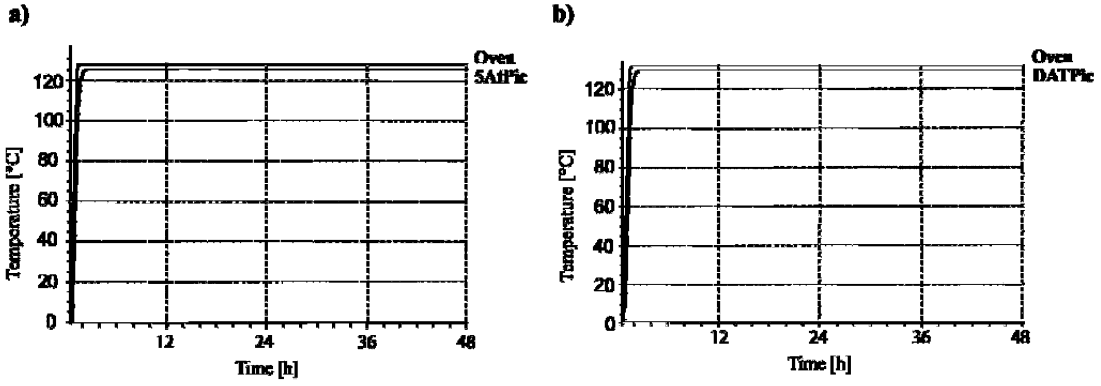

Figure 13. Thermal safety calorimetry (TSC) plots for a) **1** and b) **6**.

values above 1000 cal g^{-1}, and are higher for the more endothermic compounds **6**, **7** and **8** (>1200 cal g^{-1}) and comparable to those of TNT and PicH.

The long-term stabilities of the two highest-performing picrate salts in this study (i.e., **1** and **6**) were measured with a Systag FlexyTSC (thermal safety calorimetry) machine[52] in combination with a RADEX V5 oven and SysGraph software. The tests were run on ca. 500 mg of the pure picrate samples in glass test-vessels at atmospheric pressure. The substances were tempered at ca. 50 °C below their decomposition temperature for 48 h. Figure 13 shows the TSC plots for both compounds, together with the oven curve. The TSC curves for both pure materials are identical to that of the oven (i.e., the substances are stable over the measurements). This can be extrapolated to estimate the long-term stability at room temperature (r.t.). Under the test conditions, **1** and **6** are expected to be stable for longer than 50 years at room temp. We conclude then, that both materials show excellent long-term stabilities, which is the basic requirement for possible application.

Conclusions

We have successfully synthesized and fully characterized (analytically and spectroscopically) a new family of picrate salts with triazolium and tetrazolium cations. A full description of the ^{15}N NMR shifts and PIS/MIS values is given, which helps to determine the protonation/methylation site unequivocally without the need for expensive equipment. When suitable, the crystal structures of the compounds were determined by X-ray diffraction techniques, and a complete description of the hydrogen-bonding patterns in the structure, based on graph-set analysis, is given. Energetic testing on the sensitivities of the compounds towards impact and friction revealed insensitive picrate salts (i >40 J, f >360 N), which is advantageous in relation to picric acid. DSC analysis showed highly thermally stable compounds [e.g., T_d(**5**) = 278 °C] with melting points relatively close to the decomposition temperatures. Bomb calorimetry measurements were used to determine the heats of formation of all materials and the results were verified by means of MP2 electronic energy calculations. Calculation of the detonation parameters by use of the EXPLO5 code predicted performance values higher than those of TNT and in many cases comparable or higher than those of picric acid. The ICT code for predicting decomposition gases anticipates larger amounts of environmentally friendly nitrogen gas with less carbon soot residue than TNT, which puts into perspective the fact that classical nitroaromatics derive their energies from oxidation of their carbon backbones whereas azole-based energetic materials obtain their thrust from the formation of nitrogen gas. In addition, the best performing picrate salts in this study (**1** and **6**) also show excellent long-term thermal stabilities. Lastly, the

compounds described here are interesting examples of intermediates between classical nitroaromatic explosives and nitrogen-rich chemistry and might be of interest as prospective insensitive energetic compounds with moderate performances.

Experimental Section

Caution Note! Although we had no difficulties handling the picrate salts described here, and initial safety testing reveals decreased sensitivities for all compounds, they are nevertheless energetic materials and their explosive properties are not well established. Picric acid is sold as a water suspension and tends to detonate under certain conditions. It is recommended the synthesis be carried out only by expert personnel, wearing protective gear, using conductive equipment and on a small scale.

General: All chemical reagents and solvents were obtained from Sigma–Aldrich, Inc. or Acros Organics (analytical grade) and were used as supplied. 1-Methyl- and 5-amino-2-methyl-1*H*-tetrazole,[53] 5-amino-1,4-dimethyl-1*H*-tetrazolium iodide,[54] 5-amino-1,3-dimethyl-1*H*-tetrazolium iodide,[55] 1,5-diamino-1*H*-tetrazole,[56] 1,5-diamino-4-methyl-1*H*-tetrazolium iodide,[18d] guanazine[57] and methylguanazinium iodide[58] were prepared by previously published procedures. In addition, 5-amino-1*H*-tetrazolium picrate,[19] 1,5-diamino-1*H*-tetrazolium picrate[20a] and guanazinium picrate[59a] were synthesized by modified literature procedures as indicated below. ^{1}H, ^{13}C and ^{15}N NMR spectra were recorded on a JEOL Eclipse 400 instrument in [D$_6$]DMSO at or near 25 °C. The chemical shifts are given relative to tetramethylsilane (^{1}H, ^{13}C) or nitromethane (^{15}N) as external standards, and coupling constants are given in Hertz (Hz). Infrared (IR) spectra were recorded on a Perkin–Elmer Spectrum One FT-IR instrument as KBr pellets at 20 °C.[60] Transmittance values are qualitatively described as "very strong" (vs), "strong" (s), "medium" (m) and "weak" (w). Raman spectra were recorded on a Perkin–Elmer Spectrum 2000R NIR FT-Raman instrument fitted with a Nd:YAG laser (1064 nm). The intensities are reported as percentages of the most intense peak and are given in parentheses. Elemental analyses were performed with a Netsch Simultaneous Thermal Analyzer STA 429. Melting points were determined by differential scanning calorimetry (Linseis DSC PT-10 instrument[61] calibrated with standard pure indium and zinc). Measurements were performed at a heating rate of 5 °C min^{-1} in closed aluminium sample pans with a 1 μm hole in the top for gas release under a nitrogen flow of 20 mL min^{-1} with an empty identical aluminium sample pan as a reference.

Bomb Calorimetry: For the calorimetric measurements of the picrate salts, a Parr 1356 bomb calorimeter (static jacket) fitted with a Parr 207A oxygen bomb for the combustion of highly energetic materials was used.[62] A Parr 1755 printer, furnished with the Parr 1356 calorimeter, was used to produce a permanent record of all activities in the calorimeter. The samples (ca. 200 mg each) were carefully mixed with analytical grade benzoic acid (ca. 800 mg) and carefully pressed into pellets, which were subsequently burned in pure oxygen (3.05 MPa). The experimentally determined constant volume energies of combustion were obtained as the averages of five single measurements with standard deviations calculated as a measure of experimental uncertainty. The calorimeter was calibrated by the combustion of certified benzoic acid in oxygen at a pressure of 3.05 MPa.

5-Amino-1*H*-tetrazolium Picrate (1): Picric acid (1.035 g, 4.52 mmol) was dissolved in methanol (60 mL), giving a bright yellow solution, and was treated with neat anhydrous 5-amino-1*H*-tetrazole (0.372 g, 4.38 mmol) at 60 °C for 32 h. At this point the solvent was stripped by rotary evaporator at 40 °C and 100 mbar to give a yellow oil, which became solid under high vacuum (10^{-3} mbar). The crude product was recrystallized from a methanol/dichloromethane mixture (1:2, 8 mL), and the pure compound separated as a crystalline solid on cooling overnight (0.723 g). The solvent was then stripped again and the crude compound was recrystallized a second time from the same solvent. The crystalline compound that separated from the cold solution (0.381 g) was pure by elemental analysis and was combined with the first fraction (1.104 g, 80%). m.p. (uncorrected): 147.2–148.5 °C; DSC (5 °C min^{-1}, °C): 148 (m.p.), >175 (non-explos. dec.). ^{1}H NMR ([D$_6$]DMSO, 400.18 MHz, 25 °C, TMS): δ = 10.13 (broad, 4 H, NH/NH$_2$), 8.56 (s, 2 H, arom. H) ppm. ^{13}C{1H} NMR ([D$_6$]-DMSO, 100.63 MHz, 25 °C, TMS): δ = 160.6 (1 C, C-1), 155.0 (C–NH$_2$), 141.8 (2 C, C-2), 125.3 (2 C, C-3), 124.8 (1 C, C-4) ppm. ^{14}N NMR ([D$_6$]DMSO, 28.92 MHz, 25 °C, MeNO$_2$): δ = –12 ($\Delta\nu_{1/2}$ = 170 Hz, NO$_2$) ppm. ^{15}N NMR ([D$_6$]DMSO, 40.55 MHz, 25 °C, MeNO$_2$): δ = –12.0 (2 N, NAO$_2$), –15.2 (1 N, NBO$_2$), –27.4 (2 N, N-2/N-3), –168.1 (2 N, N-1/N-4), –326.2 (t, ^1J = 86.9 Hz, 1 N, N-5) ppm. Raman (rel. int.): $\tilde{\nu}$ = 3030 (3) 1559 (35) 1488 (16) 1366 (32) 1324 (81) 1296 (100) 1164 (21) 1090 (28) 945 (17) 913 (7) 828 (35) 750 (18) 417 (9) 344 (20) cm^{-1}. IR (KBr, rel. int.): $\tilde{\nu}$ = 3382 (s) 3250 (m) 3078 (m) 1706 (vs) 1636 (vs) 1580 (m) 1565 (s) 1484 (m) 1432 (m) 1364 (m) 1336 (vs) 1317 (s) 1267 (s) 1159 (m) 1079 (m) 1055 (m) 1027 (m) 992 (w) 944 (w) 925 (w) 911 (w) 830 (w) 791 (w) 745 (m) 716 (w) 703 (w) 625 (w) 547 (w) cm^{-1}. MS (FAB+, xenon, 6 keV, *m*-NBA matrix): *m*/*z* = 73.1 (72), 86.1 [CH$_4$N$_5$]$^+$ (100), 171.2 [(CH$_3$N$_5$)$_2$H]$^+$ (18), 207.2 (9), 221.2 (7), 239.2 (29), 327.1 (4). MS (FAB–, xenon, 6 keV, *m*-NBA matrix): *m*/*z* = 212.0 [C$_6$H$_2$N$_3$O$_6$]$^-$ (31), 228.0 [C$_6$H$_2$N$_3$O$_7$]$^-$ (100), 313.0 (17), 381.0 (3). C$_7$H$_6$N$_8$O$_7$ (314.17 g mol^{-1}): calcd. C 26.76, H 1.92, N 35.67; found C 26.76, H 2.08, N 35.72.

5-Amino-1-methyl-1*H*-tetrazolium Picrate (2): The compound was synthesized as described in ref.[59b] in a 93% yield. The elemental analysis and NMR shifts matched the reported values. 1H NMR ([D$_6$]DMSO, 400.18 MHz, 25 °C, TMS): δ = 8.58 (s, 2 H, arom. H), 5.64 (broad, 3 H, NH/NH$_2$) 3.72 (s, 3 H, CH$_3$) ppm; ^{13}C{1H} NMR ([D$_6$]DMSO, 100.63 MHz, 25 °C, TMS): δ = 160.4 (1 C, C-1), 155.0 (1 C, C–NH$_2$), 141.7 (2 C, C-2), 125.1 (2 C, C-3), 124.7 (1 C, C-4), 31.9 (1 C, CH$_3$) ppm. C$_8$N$_8$H$_8$O$_7$ (328.20 g mol^{-1}): calcd. C 29.28, H 2.46, N 34.14; found C 29.44, H 2.61, N 34.30.

5-Amino-2-methyl-1*H*-tetrazolium Picrate (3): 5-Amino-2-methyl-1*H*-tetrazole (0.220 g, 2.2 mmol) was dissolved in water (5 mL) and added to a solution of picric acid (0.512 g, 2.2 mmol) in the same solvent (5 mL) at 60 °C. The reaction mixture was brought to boiling and allowed to react for 2 h at this temperature. After this time, the solvent was stripped by rotary evaporator, and the crude product was recrystallized from a minimum amount of hot water. The product separated as a dark yellow powder, which was filtered under vacuum and washed with a little cold ethanol and then ether. The dry compound was pure by elemental analysis (0.502 g, 75%). m.p. (uncorrected): 161.6–163.4 °C; DSC (5 °C min^{-1}, °C): 161 (m.p.), 242 (non-explos. dec.). ^{1}H NMR ([D$_6$]DMSO, 400.18 MHz, 25 °C, TMS): δ = 8.60 (s, 2 H, arom. H), 5.43 (broad, 3 H, NH/NH$_2$) 4.07 (s, 3 H, CH$_3$) ppm. ^{13}C{1H} NMR ([D$_6$]DMSO, 100.63 MHz, 25 °C, TMS): δ = 167.1 (1 C, C–NH$_2$), 160.5 (1 C, C-1), 141.8 (2 C, C-2), 125.2 (2 C, C-3), 124.7 (1 C, C-4), 38.8 (1 C, CH$_3$) ppm. ^{15}N NMR ([D$_6$]DMSO, 40.55 MHz, 25 °C, MeNO$_2$): δ = –9.0 (q, J = 1.4 Hz, 1 N, N-2), –11.9 (2 N, NAO$_2$), –15.1 (1 N, NBO$_2$), –89.2 (s, 1 N, N-3) –114.4 (s, 1 N, N-1 or N-4), –114.9 (s, 1 N, N-4 or N-1), –339.1 (s, 1 N, N5H2) ppm. Raman (rel. int.): $\tilde{\nu}$

= 3107 (2) 2961 (3) 1633 (7) 1612 (7) 1562 (12) 1530 (15) 1346 (100) 1279 (26) 1178 (21) 1087 (4) 942 (13) 832 (25) 649 (5) 401 (7) 350 (9) 329 (11) 208 (8) cm^{-1}. IR (KBr, rel. int.): $\tilde{\nu}$ = 3373 (m) 3302 (m) 3214 (m) 3104 (m) 2958 (w) 2923 (w) 1696 (s) 1630 (s) 1607 (s) 1572 (w) 1562 (m) 1548 (s) 1527 (s) 1502 (m) 1468 (w) 1440 (m) 1428 (s) 1409 (m) 1391 (w) 1339 (s) 1313 (s) 1261 (s) 1204 (m) 1177 (m) 1148 (m) 1086 (s) 1016 (m) 941 (w) 918 (s) 832 (w) 808 (w) 783 (m) 763 (s) 701 (s) 647 (s) cm^{-1}. MS (FAB+, xenon, 6 keV, *m*-NBA matrix): *m*/*z* = 100.1 $[C_2H_6N_5]^+$ (100), 115.1 (18), 253.2 (15). MS (FAB-, xenon, 6 keV, *m*-NBA matrix): *m*/*z* = 212.0 $[C_6H_2N_3O_6]^-$ (39), 228.0 $[C_6H_2N_3O_7]^-$ (100), 381.0 (6). $C_8N_8H_8O_7$ (328.20 $g\,mol^{-1}$): calcd. C 29.28, H 2.46, N 34.14; found C 29.22, H 2.51, N 33.81.

5-Amino-1,4-dimethyl-1*H*-tetrazolium Picrate (4): The compound was synthesized as described in ref.[59b] in a 81% yield. The elemental analysis and NMR shifts matched the reported values. ^1H NMR ([D$_6$]DMSO, 400.18 MHz, 25 °C, TMS): δ = 9.19 (broad, 2 H, NH_2), 8.64 (s, 2 H, arom. H), 3.93 (s, 6 H, CH_3) ppm. $^{13}C\{^1H\}$ NMR ([D$_6$]DMSO, 100.63 MHz, 25 °C, TMS): δ = 160.5 (1 C, C-1), 148.5 (C–NH_2), 141.7 (2 C, C-2), 125.1 (2 C, C-3), 124.3 (1 C, C-4), 33.9 (2 C, CH_3) ppm. $C_9H_{10}N_8O_7$ (342.25 $g\,mol^{-1}$): calcd. C 31.59, H 2.94, N 32.74; found C 31.64, H 2.87, N 32.92.

5-Amino-1,3-dimethyl-1*H*-tetrazolium Picrate (5): The compound was synthesized as described in ref.[59b] in a 85% yield. The elemental analysis and NMR shifts matched the reported values. ^1H NMR ([D$_6$]DMSO, 400.18 MHz, 25 °C, TMS): δ = 8.55 (s, 2 H, arom. H), 8.17 (broad, 2 H, NH_2), 4.34 (s, 3 H, N3–CH_3), 3.95 (s, 3 H, N1–CH_3) ppm. $^{13}C\{^1H\}$ NMR ([D$_6$]DMSO, 100.63 MHz, 26.1 °C, TMS): δ = 160.8 (1 C, C-1), 158.1 (1 C, C–NH_2), 141.7 (2 C, C-2); 125.3 (1 C, C-3), 124.6 (1 C, C-4), 42.6 (1 C, N3–CH_3), 34.1 (1 C, N1–CH_3) ppm. $C_9H_{10}N_8O_7$ (342.20 $g\,mol^{-1}$): calcd. C 31.59, H 2.94, N 32.74; found C 31.65, H 2.98, N 32.54.

1,5-Diamino-1*H*-tetrazolium Picrate (6): 1,5-Diamino-1*H*-tetrazole (0.500 g, 5.00 mmol) was added to a solution containing an equivalent amount of picric acid (1.146 g, 5.00 mmol) in ethanol (60 mL), forming a bright yellow suspension. The reaction mixture was stirred for 20 h at 70 °C and left to cool slowly. Yellow crystals of the product started to separate after a short time and were filtered off and washed with diethyl ether, yielding a first crop of the compound (0.889 g). The filtrate was rotavaporated to dryness, and the crude product was recrystallized from ethanol (20 mL) to give a second crop, which was combined with the first (1.269 g, 77%). No further purification was necessary. m.p. (uncorrected): 169.1–170.4 °C; DSC (5 °C min^{-1}, °C): 170 (m.p.), 174 (dec.), ca. 250 (dec.). ^1H NMR ([D$_6$]DMSO, 400.18 MHz, 25 °C, TMS): δ = 8.59 (s, 2 H, arom. H), 8.00 (5 H, broad, NH/NH_2) ppm. $^{13}C\{1H\}$ NMR ([D$_6$]DMSO, 100.63 MHz, 25 °C, TMS): δ = 160.7 (1 C, C-1), 153.1 (1 C, C–NH_2), 142.0 (2 C, C-2), 125.5 (2 C, C-3), 125.2 (1 C, C-4) ppm. ^{14}N NMR ([D$_6$]DMSO, 28.92 MHz, 25 °C, $MeNO_2$): δ = –12 ($\Delta\nu_{1/2}$ = 180 Hz, NO_2) ppm. ^{15}N NMR ([D$_6$]-DMSO, 40.55 MHz, 25 °C, $MeNO_2$): δ = –11.7 (2 N, NAO_2), –14.8 (1 N, NBO_2), –20.9 (1 N, N-2), –35.8 (1 N, N-3), –165.6 (1 N, N-1), –173.8 (1 N, N-4), –320.1 (1 N, N6H2), –330.2 (1 N, N-5) ppm. Raman (rel. int.): $\tilde{\nu}$ = 3017 (2) 1549 (28) 1482 (11) 1369 (53) 1355 (41) 1334 (83) 1348 (100) 1270 (72) 1166 (18) 1087 (15) 950 (12) 940 (23) 915 (7) 823 (54) 780 (12) 716 (5) 335 (18) 309 (11) 212 (9) cm^{-1}. IR (KBr, rel. int.): $\tilde{\nu}$ = 3385 (s) 3307 (m) 3257 (m) 3069 (m) 1876 (w) 1722 (vs) 1634 (s) 1612 (s) 1581 (s) 1563 (s) 1536 (s) 1482 (s) 1429 (s) 1366 (s) 1334 (vs) 1271 (vs) 1165 (s) 1127 (m) 1085 (s) 997 (m) 940 (m) 913 (m) 869 (s) 794 (m) 779 (w) 749 (w) 707 (s) 691 (m) 660 (w) 518 (m) 479 (m) cm^{-1}. MS (FAB+, xenon, 6 keV, *m*-NBA matrix): *m*/*z* = 101.1 $[CH_5N_6]^+$ (30), 167.1 (7), 254.2 (12). MS (FAB–, xenon, 6 keV, *m*-NBA matrix): *m*/*z* = 211.9 $[C_6H_2N_3O_6]^-$ (28), 227.9 $[C_6H_2N_3O_7]^-$ (92), 253.0 (7), 380.9 (8). $C_7H_7N_9O_7$ (329.19 $g\,mol^{-1}$): calcd. C 25.54, H 2.14, N 38.29; found C 25.27, H 2.12, N 38.42.

1,5-Diamino-4-methyl-1*H*-tetrazolium Picrate (7): Picric acid (0.899 g, 3.93 mmol) was dissolved in boiling water (15 mL) and treated with a solution of MeDATI (0.950 g, 3.93 mmol) in water (7 mL) at room temperature. The reaction mixture was stirred for 25 min. and left to cool overnight. Large crystals of picric acid (0.323 g) separated upon cooling and were filtered off and kept for another reaction. Filtration resulted in cloudiness in the solution and eventual precipitation of a yellow powder, which was filtered off and left to air-dry. The compound was identified as the desired product and no further purification was necessary (0.692 g, 51%). DSC (5 °C min^{-1}, °C): 148 (m.p.), 154 (dec.). ^1H NMR ([D$_6$]-DMSO, 400.18 MHz, 25 °C, TMS): δ = 8.97 (2 H, broad, N–NH_2); 8.57 (s, 2 H, arom. H), 7.02 (2 H, broad, C–NH_2), 3.84 (s, 3 H, CH_3) ppm. $^{13}C\{^1H\}$ NMR ([D$_6$]DMSO, 100.63 MHz, 25 °C, TMS): δ = 160.7 (1 C, C-1), 147.4 (1 C, C–NH_2), 141.8 (2 C, C-2), 125.1 (2 C, C-3), 124.1 (1 C, C-4), 39.6 (1 C, CH_3) ppm. ^{14}N NMR ([D$_6$]DMSO, 28.92 MHz, 25 °C, $MeNO_2$): δ = –14 ($\Delta\nu_{1/2}$ = 175 Hz, NO_2) ppm. ^{15}N NMR ([D$_6$]DMSO, 40.55 MHz, 25 °C, $MeNO_2$): δ = –11.8 (2 N, NAO_2), –14.5 (1 N, NBO_2), –24.2 (1 N, N-2), –36.0 (q, ^3J = 2.0 Hz, 1 N, N-3), –168.1 (t, ^2J = 1.8 Hz, 1 N, N-1), –186.9 (q, ^2J = 2.0 Hz, 1 N, N-4), –312.1 (t, ^1J = 75.9 Hz, 1 N, N6H2), –323.8 (1 N, N5H2) ppm. Raman (rel. int.): $\tilde{\nu}$ = 3425 (2) 3076 (3) 2966 (3) 1607 (7) 1568 (22) 1547 (21) 1487 (11) 1433 (12) 1372 (41) 1337 (100) 1316 (67) 1300 (42) 1270 (47) 1163 (20) 1085 (7) 944 (15) 920 (6) 888 (4) 825 (51) 794 (15) 766 (5) 719 (7) 602 (6) 545 (5) 399 (7) 368 (10) 331 (18) 287 (8) 202 (11) cm^{-1}. IR (KBr, rel. int.): $\tilde{\nu}$ = 3357 (s) 3236 (s) 3188 (s) 3118 (s) 3048 (s) 1866 (vw) 1711 (s) 1634 (s) 1612 (s) 1563 (s) 1544 (s) 1495 (s) 1484 (m) 1431 (m) 1368 (s) 1334 (vs) 1269 (vs) 1162 (m) 1082 (m) 1037 (w) 1006 (vw) 964 (w) 936 (w) 913 (m) 839 (vw) 795 (w) 788 (w) 751 (w) 746 (w) 710 (m) 664 (vw) 635 (vw) 574 (w) 547 (w) 527 (vw) cm^{-1}. MS (FAB+, xenon, 6 keV, *m*-NBA matrix): *m*/*z* = 115.1 $[C_2H_7N_6]^+$ (100), 268.2 (14), 421.2 (2). MS (FAB–, xenon, 6 keV, *m*-NBA matrix): *m*/*z* = 212.0 $[C_6H_2N_3O_6]^-$ (18), 227.9 $[C_6H_2N_3O_7]^-$ (100), 381.0 (6). $C_8H_9N_9O_7$ (343.21 $g\,mol^{-1}$): calcd. C 28.00, H 2.64, N 36.73; found C 27.77, H 2.56, N 36.55.

3,4,5-Triamino-1,2,4-triazolium Picrate (8): 3,4,5-Triamino-1,2,4-triazolium bromide (0.867 g, 4.45 mmol) was dissolved in water (25 mL) and treated with neat picric acid (1.018 g, 4.44 mmol), producing immediate precipitation of the product. The reaction mixture was stirred at reflux for 1 h and left to cool. The product was then filtered off, washed with a little water and ethanol and left to air-dry. The compound was obtained as a yellow powder and no further purification was necessary (1.326 g, 87%). The elemental analysis and NMR shifts matched the reported values. ^1H NMR ([D$_6$]DMSO, 400.18 MHz, 25 °C, TMS): δ = 8.60 (s, 2 H, arom. H), 7.03 (broad, 4 H, N–NH_2), 5.56 (broad, 2 H, C–NH_2) ppm. $^{13}C\{^1H\}$ NMR ([D$_6$]DMSO, 100.63 MHz, 25 °C, TMS): δ = 161.2 (1 C, C-1), 150.5 (1 C, C–NH_2), 142.2 (2 C, C-2), 125.7 (2 C, C-3), 124.7 (1 C, C-4) ppm. $C_8H_9N_9O_7$ (343.21 $g\,mol^{-1}$): calcd. C 28.00, H 2.64, N 36.73; found C 27.88, H 2.68, N 36.53.

3,4,5-Triamino-1-methyl-1,2,4-triazolium Picrate (9): The compound was synthesized as described in ref.[59b] in a 90% yield. The elemental analysis and NMR shifts matched the reported values. ^1H NMR ([D$_6$]DMSO, 400.18 MHz, 25 °C, TMS): δ = 8.61 (s, 2 H, arom. H), 7.90 (broad, 2 H, N6H2), 6.48 (broad, 2 H, N5H2), 5.65 (broad, 2 H, N4H2), 3.41 (s, 3 H, CH_3) ppm. $^{13}C\{^1H\}$ NMR ([D$_6$]DMSO, 100.63 MHz, 25 °C, TMS): δ = 161.1 (1 C, C-1), 150.6

(1 C, C-N4H2), 147.7 (1 C, C-N5H2), 141.7 (2 C, C-2), 125.5 (2 C, C-3), 125.0 (1 C, C-4), 34.4 (1 C, CH_3) ppm. $C_9H_{11}N_9O_7$ (353.24 g mol^{-1}): calcd. C 30.26, H 3.10, N 35.29; found C 30.19, H 3.09, N 35.21.

Supporting Information (see also the footnote on the first page of this article): The results of the graph-set analysis, MP2 calculations and calculations of the explosive properties of mixtures of picrate salts **1**–**9** with an oxidizer can be found in the Supporting Information.

Acknowledgments

Financial support of this work by the Ludwig-Maximilian University of Munich (LMU), the Fonds der Chemischen Industrie (FCI), the European Research Office (ERO) of the U.S. Army Research Laboratory (ARL) and ARDEC (Armament Research, Development and Engineering Center) under contract nos. N 62558-05-C-0027, R&D 1284-CH-01, R&D 1285-CH-01, 9939-AN-01, W911NF-07-1-0569, W911NF-08-1-0372 and W911NF-08-1-0380 and the Bundeswehr Research Institute for Materials, Explosives, Fuels and Lubricants (WIWEB) under contract nos. E/E210/4D004/X5143 & E/E210/7D002/4F088 is gratefully acknowledged. The authors acknowledge collaborations with Dr. Mila Krupka (OZM Research, Czech Republic) in the development of new testing and evaluation methods for energetic materials and with Dr. Muhamed Sucesca (Brodarski Institute, Croatia) in the development of new computational codes to predict the detonation parameters of high-nitrogen explosives. We are indebted to and thank Dr. Betsy M. Rice (ARL, Aberdeen, Proving Ground, MD) and Dr. Gary Chen (ARDEC, Picatinny Arsenal, NJ) for many helpful and inspired discussions and support of our work. We also thank Prof. Konstantin Karaghiosoff for collecting the X-ray data and Ms. Susanne Scheutzow, M.Sc., for recording the FlexyTSC spectra.

[1] a) D. Adam, G. Holl, T. M. Klapötke, *Heteroat. Chem.* **1999**, *10*, 548–553; b) A. Hammerl, T. M. Klapötke, H. Nöth, M. Warchhold, G. Holl, M. Kaiser, U. Ticmanis, *Inorg. Chem.* **2001**, *40*, 3570–3575; c) T. M. Klapötke, H.-G. Ang, *Propell. Explos. Pyrotech.* **2001**, *26*, 221–224; d) L. Y. Bruney, T. M. Bledson, D. L. Strout, *Inorg. Chem.* **2003**, *42*, 8117–8120; e) Y.-H. Ding, S. Inagaki, *Chem. Lett.* **2003**, *32*, 304–305.

[2] a) T. M. Klapötke, P. Mayer, A. Schulz, J. J. Weigand, *Propell. Explos. Pyrotech.* **2004**, *29*, 325–332; b) D. L. Strout, *J. Phys. Chem. A* **2004**, *108*, 10911–10916; c) M. H. V. Huynh, M. A. Hiskey, E. L. Hartline, D. P. Montoya, R. Gilardi, *Angew. Chem.* **2004**, *116*, 5032–5036; *Angew. Chem. Int. Ed.* **2004**, *43*, 4924–4928; d) R. Haiges, S. Schneider, T. Schroer, K. O. Christe, *Angew. Chem.* **2004**, *116*, 5027–5032; *Angew. Chem. Int. Ed.* **2004**, *43*, 4919–4924.

[3] a) R. P. Singh, R. D. Verma, D. T. Meshri, J. M. Shreeve, *Angew. Chem.* **2006**, *118*, 3664–3682; *Angew. Chem. Int. Ed.* **2006**, *45*, 3584–3601; b) T. M. Klapötke, *Structure and Bonding*, Springer, Berlin/Heidelberg, Germany, **2007**, *125*, pp. 85–121; c) G. Drake, *US-A 6509473*, **2003**; d) G. Drake, T. Hawkins, *AFOSR Ionic Liquids Workshop* **2002**; e) V. A. Dulles, G. Drake, *AFOSR Ionic Liquids Workshop* **2003**, Aberdeen, MD.

[4] a) H. Xue, Y. Gao, B. Twamley, J. M. Shreeve, *Chem. Mater.* **2005**, *17*, 191–198; b) H. Xue, S. W. Arritt, B. Twamley, J. M. Shreeve, *Inorg. Chem.* **2004**, *43*, 7972–7977; c) Y. Gao, S. W. Arritt, B. Twamley, J. M. Shreeve, *Inorg. Chem.* **2005**, *44*, 1704–1712; d) C. F. Ye, J. M. Shreeve, *Chem. Commun.* **2005**, 2570–2572; e) H. Xue, Y. Gao, B. Twamley, J. M. Shreeve, *Inorg. Chem.* **2005**, *44*, 5068–5072; f) H. Xue, B. Twamley, J. M. Shreeve, *J. Mater. Chem.* **2005**, *15*, 3459–3465; g) H. Xue, Y. Gao, B. Twamley, J. M. Shreeve, *Inorg. Chem.* **2005**, *44*, 7009–7013.

[5] a) H. Gao, C. Ye, R. W. Winter, G. L. Gard, M. E. Sitzmann, J. M. Shreeve, *Eur. J. Inorg. Chem.* **2006**, *15*, 3221–3226; b) Y. Gao, C. F. Ye, B. Twamley, J. M. Shreeve, *Chem. Eur. J.* **2006**, *12*, 9010–9018; c) G. Gao, R. Wang, B. Twamley, M. A. Hiskey, J. M. Shreeve, *Chem. Commun.* **2006**, 4007–4009; d) Y. Huang, H. Gao, B. Twamley, J. M. Shreeve, *Eur. J. Inorg. Chem.* **2007**, 2025–2030; e) R. W. Wang, H. Gao, C. Ye, B. Twamley, J. M. Shreeve, *Inorg. Chem.* **2007**, *46*, 932–938.

[6] a) G. Kaplan, G. Drake, K. Tollison, L. Hall, T. Hawkins, *J. Heterocycl. Chem.* **2005**, *42*, 19–27; b) H. Oestmark, *Proceedings of the 9th Seminar on New Trends in the Research of Energetic Materials*, Pardubice, Czech Republic, April 19–21, **2006**, Institute of Energetic Materials, University of Pardubice, Pardubice, Czech Republic.

[7] a) J. Uddin, V. Barone, G. E. Scuseria, *Mol. Phys.* **2006**, *104*, 745–749; b) H. Oestmark, S. Walin, P. Goede, *Cent. Eur. J. Energ. Mater.* **2007**, *4*, 83–108.

[8] L. Borne, M. Herrmann, C. B. Skidmore, *Microstructure and Morphology in Energetic Materials–Particle Processing and Characterization*, Wiley-VCH, Weinheim, Germany **2005**, pp. 333–366.

[9] T. M. Klapötke, C. Miró Sabaté, *Insensitive Energetic Materials. Particles, Crystals, Composites ICT Symposium*, Pfinztal, Germany, March 13–14, **2007**.

[10] H. Feuer, A. T. Nielsen, *Nitro Compounds*, Wiley-VCH, Weinheim, Germany, **1990**.

[11] A. T. Nielsen, *Nitrocarbons*, Wiley-VCH, Weinheim, Germany **1995**.

[12] D. E. Chavez, M. A. Hiskey, R. D. Gilardi, *Angew. Chem. Int. Ed.* **2000**, *39*, 1861–1863.

[13] A. Hammerl, T. M. Klapötke, H. Nöth, M. Warchhold, G. Holl, M. Kaiser, *Inorg. Chem.* **2001**, *40*, 3570–3575.

[14] http://en.wikipedia.org/wiki/Trinitrotoluene.

[15] J. Köhler, R. Meyer, *Explosivstoffe*, 7th ed., Wiley-VCH, Weiheim, Germany **1991**.

[16] A. K. Sikder, N. Sikder, *J. Hazard. Mater.* **2004**, *A112*, 1–15.

[17] H. Gao, Y. Huang, C. Ye, B. Twamley, J. M. Shreeve, *Chem. Eur. J.* **2008**, *14*, 5596–5603.

[18] a) H. Xue, B. Twamley, J. M. Shreeve, *Eur. J. Inorg. Chem.* **2006**, 2959–2965; b) M. von Denffer, G. Heeb, T. M. Klapötke, G. Kramer, G. Spiess, J. M. Welch, *Propell. Explos. Pyrotech.* **2005**, *30*, 191–195; c) K. Karaghiosoff, T. M. Klapötke, P. Mayer, C. Miró Sabaté, A. Penger, J. M. Welch, *Inorg. Chem.* **2008**, *47*, 1007–1019; d) J. C. Gálvez-Ruiz, G. Holl, K. Karaghiosoff, T. M. Klapötke, K. Löhnwitz, P. Mayer, H. Nöth, K. Polborn, C. J. Rohbogner, M. Suter, J. J. Weigand, *Inorg. Chem.* **2005**, *44*, 4237–4253; e) J. C. Gálvez-Ruiz, G. Holl, K. Karaghiosoff, T. M. Klapötke, K. Löhnwitz, P. Mayer, H. Nöth, K. Polborn, C. J. Rohbogner, M. Suter, J. J. Weigand, *Inorg. Chem. (Correction)* **2005**, *44*, 5192–5192; f) Y. Gao, H. Gao, C. Piekarski, J. M. Shreeve, *Eur. J. Inorg. Chem.* **2007**, 4965–4972; g) T. M. Klapötke, C. Miró Sabaté, J. Stierstorfer, *Z. Anorg. Allg. Chem.* **2008**, in press; h) G. W. Drake, T. W. Hawkins, L. A. Hall, J. A. Boatz, A. J. Brand, *Propell. Explos. Pyrotech.* **2005**, *30*, 329–337.

[19] C. M. Jin, C. Ye, C. Piekarski, B. Twamley, J. M. Shreeve, *Eur. J. Inorg. Chem.* **2005**, 3760–3767.

[20] a) V. E. Matulis, A. S. Lyakhov, P. N. Gaponik, S. V. Voitekhovich, O. A. Ivashkevich, *J. Mol. Struct.* **2003**, *649*, 309–314; b) A. S. Lyakhov, S. V. Voitekhovich, L. S. Ivashkevich, P. N. Gaponik, *Acta Crystallogr., Sect. E* **2005**, *61*, o3645-o3647.

[21] a) S. V. Levchik, A. I. Balabanovich, O. A. Ivashkevich, A. I. Lesnikovich, P. N. Gaponik, L. Costa, *Thermochim. Acta* **1992**, *207*, 115–130; b) S. V. Levchik, A. I. Balabanovich, O. A. Ivashkevich, A. I. Lesnikovich, P. N. Gaponik, L. Costa, *Thermochim. Acta* **1993**, *225*, 53–65; c) A. I. Lesnikovich, O. A. Ivashkevich, S. V. Levchik, A. I. Balabanovich, P. N. Gaponik, A. A. Kulak, *Thermochim. Acta* **2002**, *388*, 233–251; d) A. Gao, Y. Oyumi, T. B. Brill, *Combust. Flame* **1991**, *83*, 345–352; e) S. V.

Levchik, A. I. Balabanovich, O. A. Ivashkevich, P. N. Gaponik, L. Costa, *Polym. Degrad. Stab.* **1995**, *47*, 333–344.
[22] a) M. Göbel, K. Karaghiosoff, T. M. Klapötke, C. Miró, J. M. Welch, *Proceedings of the 9th Seminar on New Trends in the Research of Energetic Materials*, Pardubice, Czech Republic, April 19–21, **2006**, Institute of Energetic Materials, University of Pardubice, Pardubice, Czech Republic; b) T. M. Klapötke, C. Miró Sabaté, A. Penger, M. Rusan, J. M. Welch, *Chem. Eur. J.* **2008**, manuscript in preparation.
[23] T. M. Klapötke, C. Miró Sabaté, J. M. Welch, *Z. Anorg. Allg. Chem.* **2008**, *634*, 857–866.
[24] N. B. Colthup, L. H. Daly, S. E. Wiberley, *Introduction to Infrared and Raman Spectroscopy*, Academic Press, Boston, USA, **1990**.
[25] E. Pretsch, P. Bühlmann, C. Affolter, A. Herrera, R. Martínez, *Determinación Estructural de Compuestos Orgánicos*, Springer Verlag Ibérica, Barcelona, Spain, **2001**.
[26] A. Garrone, R. Fruttero, C. Tironi, A. Gasco, *J. Chem. Soc. Perkin Trans. 2* **1989**, *12*, 1941–1945.
[27] G. J. Martin, M. L. Martin, J. P. Gouesnard, *^{15}N NMR Spectroscopy*, Springer, Berlin, Germany, **1981**.
[28] http://www.oxford-diffraction.com.
[29] *Programs for Crystal Structure Analysis* (rel. 97–2), G. M. Sheldrick, Institut für Anorganische Chemie der Universität, Tammanstrasse 4, 3400 Göttingen, Germany, **1998**.
[30] A. Altomare, M. C. Burla, M. Camalli, G. L. Cascarano, C. Giacovazzo, A. Guagliardi, A. G. Moliterni, G. Polidori, R. Spagna, *J. Appl. Crystallogr.* **1999**, *32*, 115–119.
[31] J. Bernstein, R. E. Davis, L. Shimoni, N. Chang, *Angew. Chem. Int. Ed. Engl.* **1995**, *34*, 1555–1573.
[32] http://www.ccdc.cam.ac.uk/support/documentation/rpluto/TOC.html.
[33] A. F. Holleman, E. Wiberg, N. Wiberg, *Lehrbuch der Anorganischen Chemie*, 101st ed., Walter de Gruyter, Berlin, Germany, **1995**.
[34] C. Darwich, T. M. Klapötke, C. Miró Sabaté, *Chem. Eur. J.* **2008**, *14*, 5756–5771.
[35] M. J. Frisch, G. W. Trucks, H. B. Schlegel, G. E. Scuseria, M. A. Robb, J. R. Cheeseman, J. A. Montgomery, T. Vreven Jr., K. N. Kudin, J. C. Burant, J. M. Millam, S. S. Iyengar, J. Tomasi, V. Barone, B. Mennucci, M. Cossi, G. Scalmani, N. Rega, G. A. Petersson, H. Nakatsuji, M. Hada, M. Ehara, K. Toyota, R. Fukuda, J. Hasegawa, M. Ishida, T. Nakajima, Y. Honda, O. Kitao, H. Nakai, M. Klene, X. Li, J. E. Knox, H. P. Hratchian, J. B. Cross, C. Adamo, J. Jaramillo, R. Gomperts, R. E. Stratmann, O. Yazyev, A. J. Austin, R. Cammi, C. Pomelli, J. W. Ochterski, P. Y. Ayala, K. Morokuma, G. A. Voth, P. Salvador, J. J. Dannenberg; V. G. Zakrzewski, S. Dapprich, A. D. Daniels, M. C. Strain, O. Farkas, D. K. Malick, A. D. Rabuck, K. Raghavachari, J. B. Foresman, J. V. Ortiz, Q. Cui, A. G. Baboul, S. Clifford, J. Cioslowski, B. B. Stefanov, G. Liu, A. Liashenko, P. Piskorz, I. Komaromi, R. L. Martin, D. J. Fox, T. Keith, M. A. Al-Laham, C. Y. Peng, A. Nanayakkara, M. Challacombe, P. M. W. Gill, B. Johnson, W. Chen, M. W. Wong, C. González, J. A. Pople, *Gaussian 03, Revision C.02*, Gaussian, Inc., Wallingford, CT, **2004**.
[36] J. A. Pople, R. A. Seeger, R. Krishnan, *Int. J. Quantum Chem.* **1977**, *11*, 149–163.
[37] a) A. K. Rick, T. H. Dunning, J. H. Robert, *J. Chem. Phys.* **1992**, *96*, 6796–6806; b) A. P. Kirk, E. W. David, T. H. Dunning, *J. Chem. Phys.* **1994**, *100*, 7410–7415.
[38] H. Xue, H. Gao, B. Twamley, J. M. Shreeve, *Chem. Mater.* **2007**, *19*, 1731–1739.
[39] H. D. B. Jenkins, D. Tudeal, L. Glasser, *Inorg. Chem.* **2002**, *41*, 2364–2367.
[40] H. D. B. Jenkins, H. K. Roobottom, J. Passmore, L. Glasser, *Inorg. Chem.* **1999**, *38*, 3609–3620.
[41] H. Gao, C. Ye, M. Piekarski, J. M. Shreeve, *J. Phys. Chem. C* **2007**, *111*, 10718–10731.
[42] M. Suceska, *Propell. Explos. Pyrotech.* **1991**, *16*, 197–202.
[43] Calculation of the oxygen balance: Ω (%) = (O – 2C – H/ 2 – *x*AO) 1600/*M*; *M* = molecular mass.
[44] Impact: insensitive >40 J, less sensitive ≥35 J, sensitive ≥4 J, very sensitive ≤3 J; friction: insensitive >360 N, less sensitive = 360 N, sensitive <360 N to >80 N, very sensitive ≤ 80 N, extremely sensitive ≤10 N. According to the UN Recommendations on the Transport of Dangerous Goods, (+) indicates: not safe for transport.
[45] http://www.bam.de.
[46] T. M. Klapötke, C. M. Rienäcker, *Propell. Explos. Pyrotech.* **2001**, *26*, 43–47.
[47] a) S. Zeman, V. Pelikán, J. C. Majzlík, *Eur. J. Energ. Mater.* **2006**, *3*, 45–51; b) D. Skinner, D. Olson, A. Block-Bolten, *Propell. Explos. Pyrotech.* **1997**, *23*, 34–42.
[48] *NIST Chemistry WebBook*, NIST Standard Reference Database Number 69 – March, **2003** Release, www version: http://webbook.nist.gov/chemistry.
[49] a) T. M. Klapötke, P. Mayer, C. Miró Sabaté, J. M. Welch, N. Wiegand, *Inorg. Chem.* **2008**, *47*, 6014–6027; b) K. E. Gutowski, R. D. Rogers, D. A. Dixon, *J. Phys. Chem. B* **2007**, *111*, 4788–4800.
[50] V. A. Ostrovskii, M. S. Pevzner, T. P. Kofman, I. V. Tselinskii, *Targets. Heterocycl. Syst.* **1999**, *3*, 467–526.
[51] a) *ICT*-Thermodynamic Code, v. 1.0, Fraunhofer-Institut für Chemische Technologie (ICT), Pfinztal, Germany, **1988**–**2000**; b) R. Webb, M. van Rooijen, *Proceedings of the 29th International Pyrotechnics Seminar* **2002**, 823–828; c) H. Bathelt, F. Volk, *27th International Annual Conference of ICT*, **1996**, *92*, 1–16.
[52] http://www.systag.ch.
[53] R. A. Henry, W. G. Finnegan, *J. Am. Chem. Soc.* **1954**, *76*, 923–924.
[54] T. M. Klapötke, K. Karaghiosoff, P. Mayer, A. Penger, J. M. Welch, *Propell. Explos. Pyrotech.* **2006**, *31*, 188–195.
[55] T. M. Klapötke, C. Miró Sabaté, M. Rusan, *Z. Allg. Anorg. Chem.* **2008**, *634*, 688–695.
[56] P. N. Gaponik, V. P. Karavai, *Chem. Heterocycl. Compd.* **1984**, *20*, 1388–1391.
[57] C. Darwich, T. M. Klapötke, M. Suceska, J. M. Welch, *Propell. Explos. Pyrotech.* **2007**, *32*, 235–243.
[58] C. Darwich, K. Karaghiosoff, T. M. Klapötke, C. Miró Sabaté, *Z. Anorg. Allg. Chem.* **2008**, *634*, 61–68.
[59] a) C. Darwich, T. M. Klapötke, C. Miró Sabaté, *Propell. Explos. Pyrotech.* **2007**, in press; b) T. M. Klapötke, C. Miró Sabaté, *Z. Anorg. Allg. Chem.* **2008**, *634*, 1017–1024.
[60] http://www.perkinelmer.com.
[61] http://www.linseis.net/html_en/thermal/dsc/dsc_pt10.php.
[62] http://www.parrinst.com.

Received: August 1, 2008
Published Online: October 27, 2008

